**Figure 5.** ^{1}H NMR spectra, recorded in D_2O, of the P(MPC$_{56}$-b-DEAm$_{44}$) at ambient temperature (a) and at 50 °C (b) demonstrating the desolvation of the DEAm block as a function of change in solution temperature and the intensity-average size distributions measured by dynamic light scattering (c) as a function of temperature highlighting the formation of aggregates.

Scheme 2. Idealized, Reversible Self-Assembly, with the Possible Formation of Either Micelles or Vesicles, of "Smart" AB Diblock Copolymers Based on PMPC
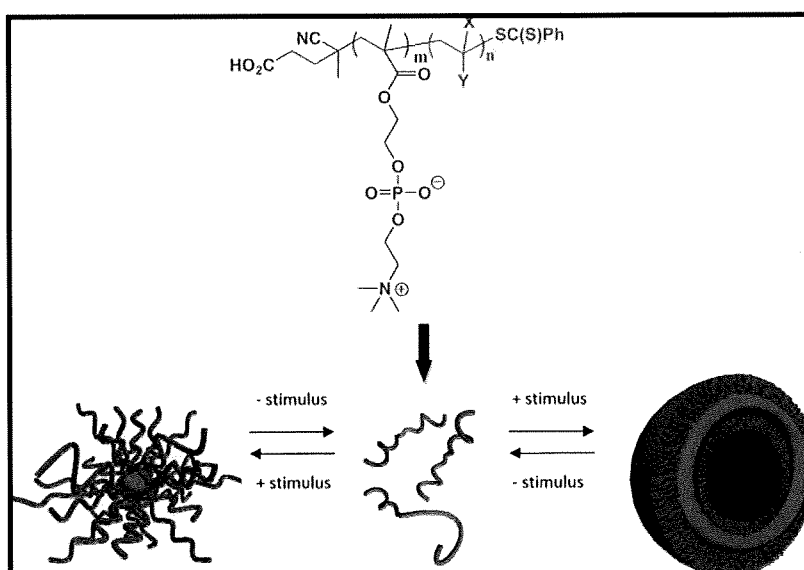
the measured size distributions for the P(MPC$_{76}$-b-DMAPS$_{24}$) copolymer in 0.5 M NaCl and deionized water at a concentration of 1 wt % at 22 °C. In the electrolyte solution unimers are observed with an average D_h of ∼6 nm. In contrast, when dissolved directly in deionized water aggregates are observed with an average D_h of 174 nm. A more detailed, fundamental study of the effect of block copolymer composition on the self-assembly properties of these copolymers is currently underway.
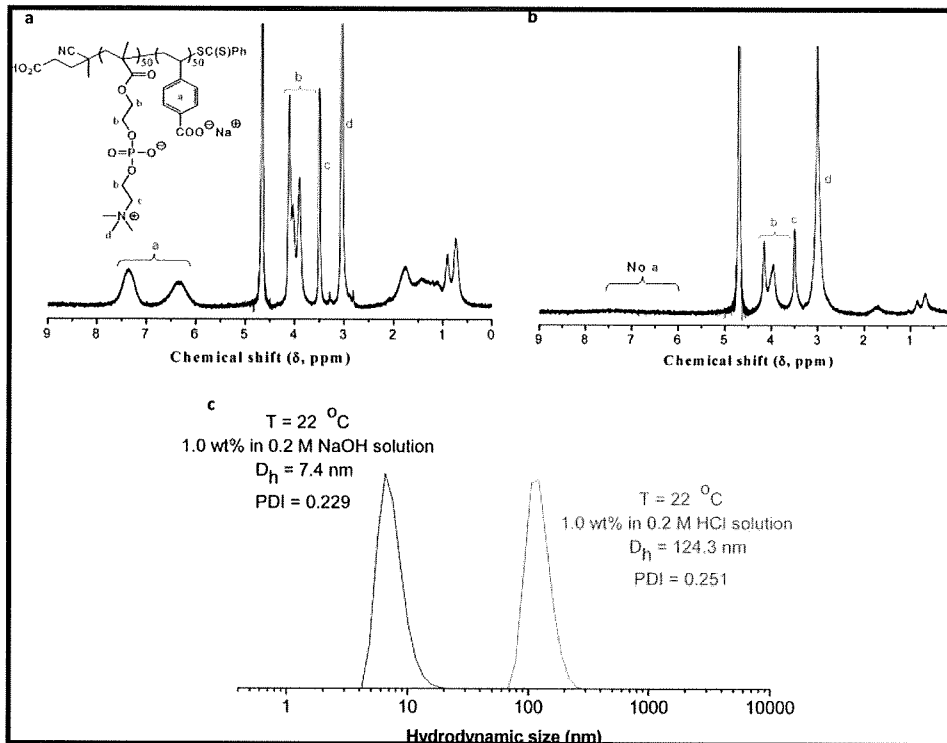
Figure 6. ^{1}H NMR spectra, recorded in D_2O, of the P(MPC$_{50}$-*b*-VBZ$_{50}$) at ambient temperature under basic conditions (a) and under acidic conditions (b), demonstrating the desolvation of the VBZ block as a function of change in solution pH and the intensity-average size distributions measured by dynamic light scattering (c) as a function of pH highlighting the formation of aggregates.

Figure 7. ^{1}H NMR spectra, recorded in D_2O, of the P(MPC$_{70}$-*b*-DnPBVA$_{30}$) at ambient temperature under acidic conditions (a) and under neutral/basic conditions (b), demonstrating the desolvation of the DnPBVA block as a function of change in solution pH and the intensity-average size distributions measured by dynamic light scattering (c) as a function of pH highlighting the formation of aggregates.
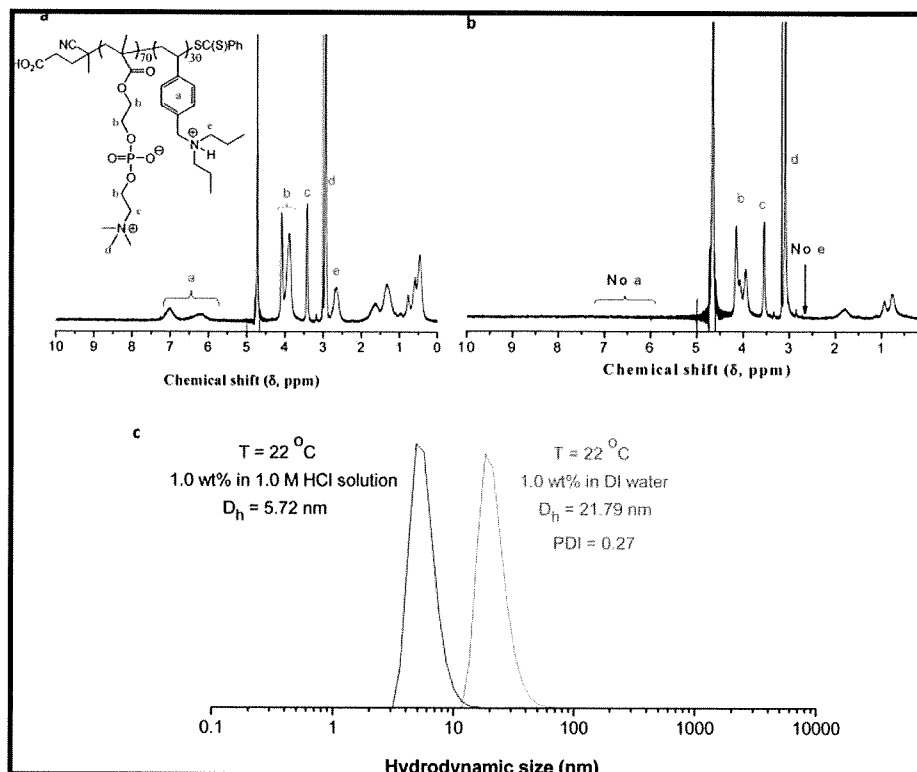
Summary and Conclusions

We have demonstrated herein that reversible addition-fragmentation chain transfer (RAFT) radical polymerization is a convenient method for the synthesis of a range of AB diblock copolymers based on the PMPC with a range of "smart" comonomers. Employing a MPC macro-CTA, well-
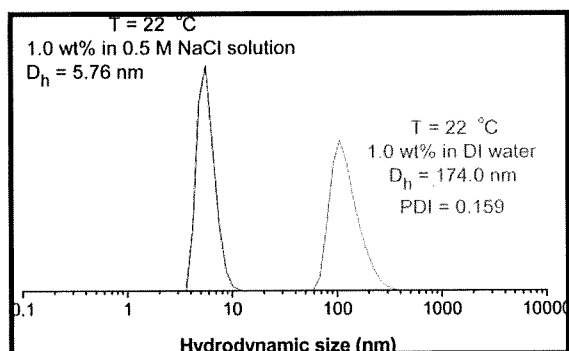
Figure 8. Experimentally determined hydrodynamic size distributions of a 1 wt % solution of the P(MPC$_{76}$-b-DMAPS$_{24}$) copolymer in 0.5 M NaCl and deionized water, demonstrating the ability to form self-assembled aggregates.

defined AB diblock copolymers of varying molar composition and narrow molecular weight distribution with N,N-diethylacrylamide, 4-vinylbenzoic acid, N,N-di-n-propylbenzylvinylamine, and N-(3-sulfopropyl)-N-methacrylooxyethyl-N,N-dimethylammonium betaine were prepared in protic media. These comonomers were chosen to yield block copolymers that were capable of undergoing stimulus induced self-assembly in aqueous media. Indeed, we demonstrated that such PMPC-based block copolymers are able to undergo self-assembly processes as a functional of either a change in solution temperature, pH, or electrolyte concentration. Preliminary evaluation of the self-assembly properties using a combination of ^{1}H NMR spectroscopy and dynamic light scattering showed that when molecularly dissolved the block copolymers had average hydrodynamic diameters in of ∼6−7 nm. In contrast, and under the appropriate applied external stimulus, aggregates in the range ∼22−180 nm. Such self-assembly is completely reversible and removal of the applied stimulus results in a return to the unimeric state.

References and Notes

(1) Lowe, A. B.; McCormick, C. L. *Chem. Rev.* **2002**, *102*, 4177–4190.
(2) Kudaibergenov, S.; Jaeger, W.; Laschewsky, A. *Adv. Polym. Sci.* **2006**, *201*, 157–224.
(3) Salamone, J. C.; Volksen, W.; Israel, S. C.; Olson, A. P.; Raia, D. C. *Polymer* **1977**, *18*, 1058–1062.
(4) Monroy Soto, V. M.; Galin, J. C. *Polymer* **1984**, *25*, 121–128.
(5) Favresse, P.; Laschewsky, A. *Polymer* **2001**, *42*, 2755–2766.
(6) Kathmann, E. E.; White, L. A.; McCormick, C. L. *Polymer* **1997**, *38*, 879–886.
(7) Bonte, N.; Laschewsky, A. *Polymer* **1996**, *37*, 2011–2019.
(8) Kathmann, E. E.; White, L. A.; McCormick, C. L. *Polymer* **1997**, *38*, 871–878.
(9) Nagaya, J.; Uzawa, H.; Minoura, N. *Macromol. Rapid Commun.* **1999**, *20*, 573–576.
(10) Ishihara, K.; Ueda, T.; Nakabayashi, N. *Polym. J.* **1990**, *22*, 355–360.
(11) Ishihara, K.; Ziats, N. P.; Tierney, B. P.; Nakabayashi, N.; Anderson, J. M. *J. Biomed. Mater. Res.* **1991**, *25*, 1397–1407.
(12) Hasegawa, T.; Iwasaki, Y.; Ishihara, K. *J. Biomed. Mater. Res.* **2002**, *63*, 333–341.
(13) Lobb, E. J.; Ma, I.; Billingham, N. C.; Armes, S. P.; Lewis, A. L. *J. Am. Chem. Soc.* **2001**, *123*, 7913–7914.
(14) Ishihara, K.; Iwasaki, Y.; Fiujiike, A.; Kurita, K.; Nakabayashi, N. *J. Polym. Sci., Part A: Polym. Chem.* **1996**, *34*, 199–205.
(15) Oishi, T.; Fukuda, T.; Uchiyama, H.; Kondou, F.; Hoe, H.; Tsutsumi, H. *Polymer* **1997**, *38*, 3109–3115.

(16) Sugiyama, K.; Ohga, K.; Aoki, H. *Macromol. Chem. Phys.* **1995**, *196*, 1907–1916.
(17) Kros, A.; Gerritsen, M.; Murk, J.; Jansen, J. A.; Sommerdijk, N. A. J. M. *J. Polym. Sci., Part A: Polym. Chem.* **2001**, *39*, 468–474.
(18) Pujol-Fortin, M.-L.; Galin, J. C. *Macromolecules* **1991**, *24*, 4523–4530.
(19) Pujol-Fortin, M.-L.; Galin, J. C. *Polymer* **1994**, *35*, 1462–1472.
(20) Chrisment, J.; Galin, M.; Galin, J. C. *New J. Chem.* **1995**, *19*, 303–311.
(21) Galin, J. C.; Galin, M. *J. Polym. Sci., Part A: Polym. Phys.* **1995**, *33*, 2033–2043.
(22) Grassl, B.; Francois, J.; Billon, L. *Polym. Int.* **2001**, *50*, 1162–1169.
(23) Ladenheim, H.; Morawetz, H. *J. Polym. Sci.* **1957**, *26*, 251–254.
(24) Hart, R.; Timmerman, D. *J. Polym. Sci.* **1958**, *28*, 638–640.
(25) Lowe, A. B.; Billingham, N. C.; Armes, S. P. *Chem. Commun.* **1996**, 1555–1556.
(26) Tuzar, Z.; Popisil, H.; Plestil, J.; Lowe, A. B.; Baines, F. L.; Billingham, N. C.; Armes, S. P. *Macromolecules* **1997**, *30*, 2509–2512.
(27) Bütün, V.; Bennett, C. E.; Vamvakaki, M.; Lowe, A. B.; Billingham, N. C.; Armes, S. P. *J. Mater. Chem.* **1997**, *7*, 1693–1695.
(28) Lowe, A. B.; Billingham, N. C.; Armes, S. P. *Macromolecules* **1999**, *32*, 2141–2148.
(29) Lowe, A. B.; Vamvakaki, M.; Wassall, M. A.; Wong, L.; Billingham, N. C.; Armes, S. P.; Lloyd, A. W. *J. Biomed. Mater. Res.* **2000**, *52*, 88–94.
(30) Ma, I.; Lobb, E. J.; Billingham, N. C.; Armes, S. P.; Lewis, A. L.; Lloyd, A. W. *Macromolecules* **2002**, *35*, 9306–9314.
(31) Ma, Y.; Tang, Y.; Billingham, N. C.; Armes, S. P.; Lewis, A. L.; Lloyd, A. W.; Salvage, J. P. *Macromolecules* **2003**, *36*, 3475–3484.
(32) Licciardi, M.; Tang, Y.; Billingham, N. C.; Armes, S. P.; Lewis, A. L. *Biomacromolecules* **2005**, *6*, 1085–1098.
(33) Kimura, M.; Takai, M.; Ishihara, K. *J. Biomed. Mater. Res.* **2007**, *80A*, 45–54.
(34) Sawada, S.-i.; Sakaki, S.; Iwasaki, Y.; Nakabayashi, N.; Ishihara, K. *J. Biomed. Mater. Res* **2003**, *64A*, 411–416.
(35) Ueda, T.; Oshida, H.; Kurita, K.; Ishihara, K.; Nakabayashi, N. *Polym. J.* **1992**, *24*, 1259–1269.
(36) Ishihara, K.; Aragaki, R.; Ueda, T.; Watenabe, A.; Nakabayashi, N. *J. Biomed. Mater. Res.* **1990**, *24*, 1069–1077.
(37) Lewis, A. L.; Hughes, P. D.; Kirkwood, L. C.; Leppard, S. W.; Redman, R. P.; Tolhurst, L. A.; Stratford, P. W. *Biomaterials* **2000**, *21*, 1847–1859.
(38) West, S. L.; Salvage, J. P.; Lobb, E. J.; Armes, S. P.; Billingham, N. C.; Lewis, A. L.; Hanlon, G. W.; Lloyd, A. W. *Biomaterials* **2004**, *25*, 1195–1204.
(39) Moro, T.; Takatori, Y.; Ishihara, K.; Konno, T.; Takigawa, Y.; Matsushita, T. *Nat. Mater.* **2004**, *3*, 829–836.
(40) Fujii, K.; Matsumoto, H.; Koyama, Y.; Iwasaki, Y.; Ishihara, K.; Takakuda, K. *J. Vet. Med. Sci.* **2008**, *70*, 167–173.
(41) Rankin, D. A.; Lowe, A. B. *Macromolecules* **2008**, *41*, 614–622.
(42) Colak, S.; Tew, G. N. *Macromolecules* **2008**, *41*, 8436–8440.
(43) Moad, G.; Rizzardo, E.; Thang, S. H. *Aust. J. Chem.* **2005**, *58*, 379–410.
(44) McCormick, C. L.; Lowe, A. B. *Acc. Chem. Res.* **2004**, *37*, 312–325.
(45) Lowe, A. B.; McCormick, C. L. *Prog. Polym. Sci.* **2007**, *32*, 283–351.
(46) Barner-Kowollik, C.; Buback, M.; Charleux, B.; Coote, M. L.; Drache, M.; Fukuda, T.; Goto, A.; Klumperman, B.; Lowe, A. B.; McCleary, J. B.; Moad, G.; Monteiro, M. J.; Sanderson, R. D.; Tonge, M. P.; Vana, P. *J. Polym. Sci., Part A: Polym. Chem.* **2006**, *44*, 5809–5831.
(47) Favier, A.; Charreyre, M.-T. *Macromol. Rapid Commun.* **2006**, *27*, 653–692.
(48) Mitsukami, Y.; Hashidzume, A.; Yusa, S.-i.; Morishima, Y.; Lowe, A. B.; McCormick, C. L. *Polymer* **2006**, *47*, 4330–4340.
(49) Lowe, A. B.; Wang, R.; Tiriveedhi, V.; Butko, P.; McCormick, C. L. *Macromol. Chem. Phys.* **2007**, *208*, 2339–2347.
(50) Wang, R.; Lowe, A. B. *J. Polym. Sci., Part A: Polym. Chem.* **2007**, *45*, 2468–2483.
(51) Lowe, A. B.; Torres, M.; Wang, R. *J. Polym. Sci., Part A: Polym. Chem.* **2007**, *45*, 5864–5871.
(52) Sumerlin, B. S.; Lowe, A. B.; Thomas, D. B.; Convertine, A. J.; Donovan, M. S.; McCormick, C. L. *J. Polym. Sci., Part A: Polym. Chem.* **2004**, *42*, 1724–1734.
(53) Gondi, S. R.; Vogt, A. P.; Sumerlin, B. S. *Macromolecules* **2007**, *40*, 474–481.
(54) Lowe, A. B.; Wang, R. *Polymer* **2007**, *48*, 2221–2230.
(55) Wang, R.; McCormick, C. L.; Lowe, A. B. *Macromolecules* **2005**, *38*, 9518–9525.

(56) Convertine, A. J; Lokitz, B. S.; Vasilieva, Y.; Myrick, L. J.; W., S. C.; Lowe, A. B.; McCormick, C. L. *Macromolecules* **2006**, *39*, 1724–1730.

(57) Chan, J. W.; Yu, B.; Hoyle, C. E.; Lowe, A. B. *Chem. Commun.* **2008**, 4959–4961.

(58) Convertine, A. J.; Lokitz, B. S.; Lowe, A. B.; Scales, C. W.; Myrick, L. J.; McCormick, C. L. *Macromol. Rapid Commun.* **2005**, *26*, 791–795.

(59) Li, M.; De, P.; Gondi, S. R.; Sumerlin, B. S. *J. Polym. Sci., Part A: Polym. Chem.* **2008**, *46*, 5093–5100.

(60) Scales, C. W.; Vasilieva, Y.; Convertine, A. J.; Lowe, A. B.; McCormick, C. L. *Biomacromolecules* **2005**, *6*, 1846–1850.

(61) Vasilieva, Y.; Scales, C. W.; Thomas, D. B.; Ezell, R. G.; Lowe, A. B.; Ayres, N.; McCormick, C. L. *J. Polym. Sci., Part A: Polym. Chem.* **2005**, *43*, 3141–3152.

(62) Pound, G.; Aguesse, F.; McCleary, J. B.; Lange, R. F. M.; Klumperman, B. *Macromolecules* **2007**, *40*, 8861–8871.

(63) Mori, H.; Ookuma, H.; Endo, T. *Macromolecules* **2008**, *41*, 6925–6934.

(64) Yasser, A.; Andreas, G.; Seema, A. *Macromol. Rapid Commun.* **2007**, *28*, 1923–1928.

(65) Arotcarena, M.; Heise, B.; Ishaya, S.; Laschewsky, A. *J. Am. Chem. Soc.* **2002**, *124*, 3787–3793.

(66) Donovan, M. S.; Sumerlin, B. S.; Lowe, A. B.; McCormick, C. L. *Macromolecules* **2002**, *35*, 8663–8666.

(67) Donovan, M. S.; Lowe, A. B.; Sanford, T. A.; McCormick, C. L. *J. Polym. Sci., Part A: Polym. Chem.* **2003**, *41*, 1262–1281.

(68) Yusa, S.-i.; Fukuda, K.; Yamamoto, T.; Ishihara, K.; Morishima, Y. *Biomacromolecules* **2005**, *6*, 663–670.

(69) Stenzel, M. H.; Barner-kowollik, C.; Davis, T. P.; Dalton, H. M. *Macromol. Biosci.* **2005**, *4*, 445–453.

(70) Mitsukami, Y.; Donovan, M. S.; Lowe, A. B.; McCormick, C. L. *Macromolecules* **2001**, *34*, 2248–2256.

(71) Gabaston, L. I.; Furlong, S. A.; Jackson, R. A.; Armes, S. P. *Polymer* **1999**, *40*, 4505–4514.

(72) Madsen, J.; Armes, S. P.; Lewis, A. L. *Macromolecules* **2006**, *39*, 7455–7457.

BM8014945
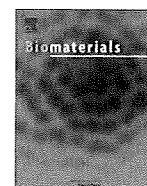
Protein adsorption and cell adhesion on cationic, neutral, and anionic 2-methacryloyloxyethyl phosphorylcholine copolymer surfaces

Yan Xu*, Madoka Takai*, Kazuhiko Ishihara

Department of Materials Engineering, School of Engineering and Center for NanoBio Integration, The University of Tokyo, 7-3-1, Hongo, Bunkyo-ku, Tokyo 113-8656, Japan

ABSTRACT

Protein adsorption and cell adhesion on cationic, neutral, and anionic water-soluble 2-methacryloyloxyethyl phosphorylcholine (MPC) copolymer surfaces were compared. These model MPC copolymers coated SiO_2 surfaces exhibited comparable surface ζ-potentials of 26.1 mV, near 0 mV, and −24.2 mV, respectively. X-ray photoelectron spectroscopy analyses indicated the similarities and the differences in the surface composition between the sample surfaces. Atomic force microscopy analyses revealed that the type of the charged moiety did not affect the surface roughness. Static contact angle measurements and dynamic contact angle analyses not only indicated that the surfaces were very hydrophilic in general, but also provided information on the surface mobility and the dominant role of MPC at the surface in aqueous conditions. Comparing with the SiO_2 substrates on which protein seriously adsorbed and cell heavily adhered, three MPC copolymers coated surfaces, despite their different charge properties, exhibited significantly low adsorbed amounts of different proteins having various electrical natures and totally no cell adhesion. This suggested that the incorporation of charged moieties in the MPC copolymers did not significantly inspire both the protein adsorption and cell adhesion. The MPC moieties were predominant at the surface when in contact with aqueous conditions and thereby dominated the bio-adsorptions, while the possible effect from electrostatic interactions would be too small and too limited to influence the overall situation. Therefore, these MPC copolymer surfaces can satisfy those biological applications requiring not only electrical but also non-biofouling properties.

© 2009 Elsevier Ltd. All rights reserved.

1. Introduction

2-Methacryloyloxyethyl phosphorylcholine (MPC) polymers have been widely used to construct non-biofouling surfaces in various biomedical applications as they have been shown to resist both protein adsorption and cell adhesion [1–3]. The MPC unit contains a zwitterionic phospholipid group (i.e. phosphorylcholine (PC)) that is also present in cell membranes and possesses non-thrombogenic property and high biocompatibility. Nevertheless, the widely researched MPC polymers are mainly electrically neutral in nature and the behaviors of protein adsorption and cell adhesion on the electrically charged MPC polymer surfaces have not been fully elucidated.

Lewis et al. have evaluated a cationic MPC copolymer and revealed its potential in the application of drug delivery systems [4]. Others have reported their achievements in the successful development of cationically charged MPC polymers as gene vectors

[5–7]. On the one hand, as decided by their purposes, these researches focused on the polymer-DNA complexes formation and the subsequent transfection, and very few touched upon the story of interactions of proteins/cells to the charged MPC polymers. However, this is an essential issue that should be addressed before they are administrated in the body: generally, charged polymers tend to nonspecifically bind proteins and cells due to the electrostatic interactions, which would cause wrong targeting and low efficiency, possibly induce their accumulation in the bloodstream and organs, and may initiate inflammatory responses of the body [8,9]; consequently, these problems seriously restrict and impede the applications of charged polymers in biomedicine. On the other hand, the components of these reported cationic MPC copolymers varied with the research topics. To elucidate the fundamental aspects such as interactions between the proteins/cells and the polymer, comparable model polymers with different electrical natures are very beneficial and necessary.

With the incorporation of an anionic monomer 3-methacryloyloxypropyl sulfonate (PMPS), we previously developed an anionic MPC copolymer, poly(MPC-co-n-butyl methacrylate (BMA)-co-PMPS-co-3-methacryloxypropyl trimethoxysilane (MPTMSi)) (referred to as PMBSSi, Fig. 1) [10]. It was revealed that the PMBSSi

* Corresponding authors. Tel.: +81 3 5841 7125; fax: +81 3 5841 8647.
E-mail addresses: xuyan@icl.t.u-tokyo.ac.jp (Y. Xu), takai@mpc.t.u-tokyo.ac.jp (M. Takai).

a PMBASi

MPC   BMA   MTAC   MPTMSi

b PMSi

MPC   MPTMSi

c PMBSSi

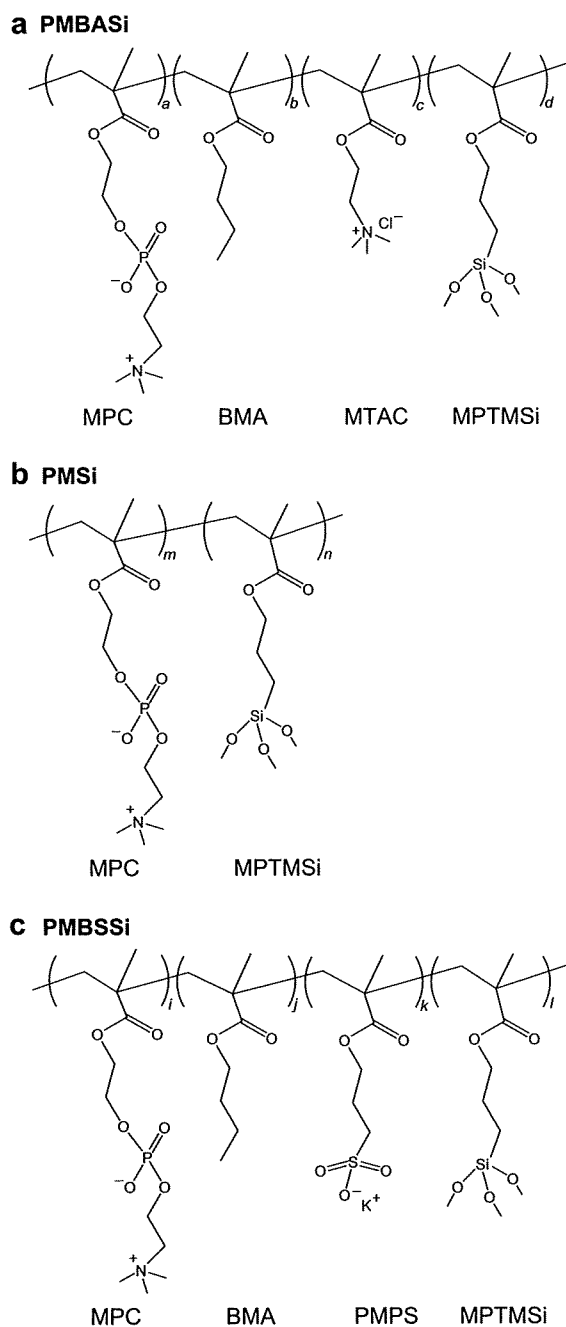MPC   BMA   PMPS   MPTMSi

Fig. 1. Chemical structures of (a) PMBASi (cationic), (b) PMSi (neutral), and (c) PMBSSi (anionic).

has high capability to suppress the protein adsorption [11]. The understanding caused us to explore whether the incorporation of cationic charge in an MPC polymer system has the same properties and merits as the incorporation of anionic charge. 2-Methacryloyloxyethyl trimethyl ammonium chloride (MTAC), which contains a cationically charged group, was therefore introduced for this purpose. MTAC was chosen because it not only has reactivity to the other methacrylate monomers such as MPC but also is commercially available and well documented in literature [12,13]. By replacing the anionic PMPS in the PMBSSi with the cationic MATC, recently we have developed a cationic MPC copolymer,

which is poly(MPC-co-BMA-co-MTAC-co-MPTMSi) and is referred to as PMBASi (Fig. 1). PMBASi and PMBSSi are comparable on the structure. Like the anionic PMBSSi, the cationic PMBASi is also composed of zwitterionic phospholipid moieties (i.e., MPC), hydrophobic moieties (i.e., BMA), charged moieties (i.e., MTAC), and covalently functional moieties (i.e., MPTMSi), which represent the basic, necessary aspects of a copolymer system and can be used as a model cationic MPC copolymer for research. For comparison, a typical neutral MPC copolymer without incorporation of charge and hydrophobic moieties, that is poly(MPC-co-MPTMSi) (referred to as PMSi, Fig. 1), was also synthesized.

Interfacial properties including surface chemistry [14,15], functional groups [16], charge [17–19], roughness [20,21], and wettability [22,23], are generally believed to be closely related to both the protein adsorption and the cell adhesion to a surface. In this study, the behaviors of protein adsorption and cell adhesion on the cationic, neutral, and anionic MPC copolymer surfaces were comparatively investigated from these interfacial aspects. We believe that the information obtained in this study is crucial and meaningful, to clarify the effect of the charge incorporation on an MPC polymer surface, to elucidate the fundamental mechanism of the protein adsorption and cell adhesion to a charged surface, and to explore the potential of the MPC polymers to be applied in the biomedical areas needing charged but non-biofouling surfaces.

2. Materials and methods

2.1. Chemicals, reagents, and proteins

2-Methacryloyloxyethyl phosphorylcholine (MPC) was synthesized as already reported by us elsewhere [1]. n-Butyl methacrylate (BMA) (Kanto chemicals, Tokyo, Japan) was distilled before use. 2-Methacryloyloxyethyl trimethylammonium chloride (MTAC) (Wako Pure Chemical, Tokyo, Japan), potassium 3-methacryloyloxypropyl sulfonate (PMPS) (Tokyo Kasei Kogyo Co., Tokyo, Japan), 3-methacryloxypropyl trimethoxysilane (MPTMSi) (Kanto Chemicals), and α,α'-azobisisobutyronitrile (AIBN) (Kanto Chemicals) were commercially purchased as a fine grade. Deuterium oxide (D_2O, 99.8% for NMR spectroscopy) and Ethanol-D (CD_3CD_2OD, 99% for NMR spectroscopy) were purchased from Merck KGaA (Darmstadt, Germany). SiO_2 substrates (thickness 0.5 mm) were obtained from Sendai Quartz and Glass (Sendai, Japan). Pepsin (35.0 kDa, $pI = 1.0$) from porcine stomach mucosa, albumin from bovine serum (BSA, 66.0 kDa, $pI = 4.7$), ribonuclease A (RNase A, 13.7 kDa, $pI = 9.5$) from bovine pancreas, and lysozyme (LYZ, 14.3 kDa, $pI = 11.0$) from chicken egg white were purchased from Aldrich–Sigma (St. Louis, MO, USA). Dulbecco's modified eagle's medium (DMEM), fetal bovine serum (FBS), Dulbecco's phosphate buffered saline (PBS, pH 7.1), and other cell culture reagents were purchased from Invitrogen (Carlsbad, CA, USA).

2.2. Synthesis and characterization of MPC copolymers

Poly (MPC-co-BMA-co-MTAC-co-MPTMSi) (PMBASi, Fig. 1) was synthesized by a conventional radical polymerization technique. Briefly, the desired amounts of MPC, BMA, MTAC, MPTMSi, and AIBN (as initiator) were first dissolved in ethanol in a polymerization flask, and then the copolymerization was performed at 60 °C for 6 h in the flask after sealed. The polymerization product was collected after a reprecipitation from an ether/chloroform (7/3, v/v) mixture solvent. The remaining solvent was removed via a vacuum drying to get a white powder. The structure was identified by ^1H NMR spectra (JEOL, 270 MHz, Tokyo, Japan) (CD_3CD_2OD, δ): $\delta_H = 0.77$–0.81 (–CH$_2$Si–), 0.90–1.09 (α-CH$_3$), 1.19–1.55 (–CH$_3$), 1.84–2.26 (–CH$_2$–), 3.00–3.17 (–N(CH$_3$)$_3$), 3.24–3.38 (–OCH$_2$CH$_2$OP), 3.69–4.44 (–OCH$_2$–).

Poly (MPC-co-MPTMSi) (PMSi, Fig. 1) was synthesized using the same method with the monomers of MPC and MPTMSi. ^1H NMR spectra (D_2O, δ): $\delta_H = 0.60$–0.65 (–CH$_2$Si–), 0.93–1.10 (α-CH$_3$), 1.14–1.46 (–CH$_2$–), 2.87–3.01 (–N(CH$_3$)$_3$), 3.54–3.70 (–OCH$_2$CH$_2$OP), 3.94–4.31 (–OCH$_2$–).

Poly (MPC-co-BMA-co-PMPS-co-MPTMSi) (PMBSSi, Fig. 1) was synthesized using the same method with the monomers of MPC, BMA, PMPS, and MPTMSi. ^1H NMR spectra (CD_3CD_2OD, δ): $\delta_H = 0.60$–0.65 (–CH$_2$Si–), 0.90–1.04 (α-CH$_3$), 1.22–1.37 (–CH$_3$), 1.56–1.83 (–CH$_2$–), 3.15–3.24 (–N(CH$_3$)$_3$), 3.46–3.68 (–OCH$_2$CH$_2$OP), 3.97–4.24 (–OCH$_2$–).

The average molecular weight was estimated by a gel permeation chromatography (GPC) system (JASCO, Tokyo, Japan). The solubility was evaluated by dissolving 0.1 g polymer powder in a 10 mL solvent (water and ethanol). The molecular properties of three polymers are summarized in Table 1.

172

Table 1
Molecular properties of PMBASi, PMSi, and PMBSSi.

Abb.	Composition (mole fraction)[a]	Molecular weight (M_w)[c]	Polydispersity ratio(M_w/M_n)[d]	Solubility[e]	
	[MPC/BMA/X[b]/ MPTMSi]			H_2O	EtOH
PMBASi	48/23/18/11	9.9×10^3	1.1	+	+
PMSi	80/0/0/20	9.7×10^3	1.1	+	+
PMBSSi	46/32/9/13	11.8×10^3	1.2	+	+

[a] Determined by ^1H NMR.
[b] X is MTAC in PMBASi or PMPS in PMBSSi.
[c] Weight average molecular weight (M_w);determined by GPC, PEO standard.
[d] M_n: number average molecular weight.
[e] Evaluated by dissolving 0.1 g polymer powder in a 10 mL solvent; +: soluble.

2.3. Preparation of covalent coating on SiO₂ substrates

The SiO₂ substrates were first cleaned by ultrasonic rinsing in ethanol and O₂ plasma treatment successively. Then, the cleaned substrates were immersed in 3.00 mg mL⁻¹ polymer ethanol solutions for 2 h. After dried under nitrogen, the coated substrates were immediately further dried in vacuo overnight. Before use, the coated substrates were thoroughly rinsed with the distilled water to remove the remaining unreacted molecules, then dried under nitrogen, and dried again in vacuo overnight.

2.4. X-ray photoelectron spectroscopy (XPS) analysis

XPS (Axis-His, Shimadzu/KRATOS, Kyoto, Japan) analyses were made under a high vacuum condition of 1×10^{-9} Torr with MgKα (1253.6 eV) X-ray source. The applied voltage was 12 kV, the electric current was 10 mA, and the employed takeoff angle was 90°. The binding energy (BE) scale was corrected using C_{1s} as a reference at BE = 285 eV. The six elements present in the polymers were identified from their XPS peaks: silicon (Si_{2p}, BE ~ 102 eV), phosphorus (P_{2p}, BE ~ 133 eV), sulfur (S_{2p}, BE ~ 168 eV), carbon (C_{1s}, BE ~ 285 eV), nitrogen (N_{1s}, BE ~ 402 eV), and oxygen (O_{1s}, BE ~ 533 eV).

2.5. Measurement of surface ζ-potential

The measurements of the surface ζ-potentials of both the coated and the uncoated SiO₂ substrates were carried out in a 10 mM NaCl solution using an electrophoretic light-scattering spectrophotometer (ELS 8000, Otsuka Electron., Osaka, Japan) with a plate cell. Six measurements were applied to each sample.

2.6. Atomic force microscopy (AFM) analysis

AFM observations were performed with a commercial instrument (Bioscope, Nanoscope IIIa, Veeco, Santa Barbara, CA, USA). Images (1.0 × 1.0 μm² area) were acquired using the tapping mode of operation with a phosphorus (n) doped silicon cantilever (RTESP). The root-mean-square (rms) roughness was obtained to quantitatively describe the roughness of the surface topography. More than three measurements for each sample were recorded to calculate the average.

2.7. Measurement of static contact angle (SCA)

The static water contact angle of the surface was measured using an automatic contact angle meter (CA-W, Kyowa Interface Science, Saitama, Japan) at room temperature. At least six different areas were measured and averaged for each sample.

2.8. Measurement of dynamic contact angle (DCA)

DCA analyses were carried out using a Cahn DCA analytical instrument (model315, ATI, Madison, USA). Both coated and uncoated SiO₂ substrates with dimensions 30 × 30 × 0.5 mm³ were prepared for measurements. The substrates were lowered into ultrapure water at a speed of 80 μm s⁻¹. The software WindDCA (Cahn Instruments Inc.) was used to record and calculate the advancing contact angle (θ_A) and the receding contact angle (θ_R). Contact angle hysteresis is $(\theta_A - \theta_R)$. The mobility factor (MF) of the surface was calculated by using the following equation: $MF = (\theta_A - \theta_R)/\theta_A$ [24].

2.9. Assessment of non-specific protein adsorption

The assessments were performed on both the coated and the uncoated SiO₂ substrates with a series of typical anionic and cationic proteins as aforementioned, according to a standard protocol as described by us elsewhere [25]. Simply, after equilibrated in water, the substrates (coated and uncoated) were immersed in 10 mL

of protein solution (0.32 g L⁻¹, prepared in PBS buffer, pH 7.1), followed by an incubation at 37 °C for 1 h. Then the substrates were rinsed twice with sufficient PBS (pH 7.1) for 5 min each while stirring at 300 rpm. To detach all the adsorbed protein from the SiO₂ substrate, each substrate was immersed in 2.0 mL of 10 mg mL⁻¹ sodium dodecyl sulfate (SDS) solution (water as solvent) in a small sealed case, followed by an ultrasonication for 10 min. The amount of protein in the SDS solution was determined by the Micro BCA (bicinchoninic acid) protocol (Micro BCA Protein Assay Kit, Pierce Biotechnology, Rockford, IL, USA).

2.10. Assessment of cell adhesion

The assessment of cell adhesion was carried out by using a mouse fibroblast cell line, L929 cells (RCB 0081, Cell Bank, Japan) as model cells. Both the coated and the uncoated SiO₂ substrates (20 × 20 × 0.5 mm³) were placed in a 60 mm cell culture dish, and then 1 mL cell suspension (cell density: 1.0×10^5 cells mL⁻¹) in DMEM supplemented with 10% fetal bovine serum (FBS) was seeded on each substrate. After 2 h of incubation at 37 °C in a humidified atmosphere of 5% CO₂, 10 mL culture medium was added to the culture dish. Together with the substrates, the cells were cultured in the incubator. Before assessment, the substrates were rinsed with the medium to wash off the unattached cells. The cell adhesion was assessed by observing the substrates with a phase-contrast microscope (IX71S1F-2, Olympus, Tokyo, Japan).

3. Results and discussion

3.1. Molecular properties of cationic, neutral, and anionic MPC polymers

Fig. 1 shows the structures of the three MPC copolymers with or without charged moieties. Their molecular properties are listed in Table 1. Besides MPC, all three copolymers contain MPTMSi which is a typical methacrylate silane-coupling agent. Silane-coupling moieties such as the MPTMSi moieties in a copolymer are very useful in many biomedical applications because they can react with various inorganic materials such as glass, silica, silicone, and metals to form a chemical bond with surface or can induce a crosslinkable coating on various organic materials such as poly(ethylene terephthalate) (PET), poly(vinyl chloride) (PVC), etc. [26]. The compositions of MPTMSi in all three copolymers are higher than 10%, a composition which has been proved sufficient for an MPC copolymer to form a stable covalent coating on a SiO₂ substrate [11]. The MTAC moieties of PMBASi and the PMPS moieties of PMBSSi are two types of methacrylate units respectively having oppositely charged groups. A serial PMBASi copolymers containing varying compositions of MTAC were synthesized and characterized. In this study, the PMBASi containing 18% mole fraction of MTAC were chosen because it had an approximately equal absolute value of ζ-potential as the available PMBSSi had. Both PMBASi and PMBSSi have hydrophobic moieties, i.e. BMA, favoring us to elucidate the role of the hydrophobic moieties in the copolymer by comparing with the super hydrophilic PMSi which has no BMA moiety. Furthermore, PMBASi and PMBSSi share another common feature as they contain almost same amounts of the MPC fraction. As shown in Table 1, all these three MPC polymers have similar molecular weights, possess narrow polydispersities, and are soluble in both water and ethanol. These molecular characteristics make the three MPC copolymers comparable and fit for a comparative investigation as model copolymers.

3.2. Interfacial properties of coatings

3.2.1. Sample surfaces

The SiO₂ (quartz) substrate was used in the study in consideration of its high purity, clear chemical structure, well-defined silane reactivity, and most importantly, wide applications as various biomaterials. To characterize the interfacial properties of these copolymers, SiO₂ substrates respectively with three copolymer covalent coatings were prepared according to a same protocol as

described in section Materials and methods. Including uncoated, PMBASi-coated, PMSi-coated, and PMBSSi-coated SiO$_2$ substrates, four sample surfaces were used in the subsequent investigations. Fig. 2 illustrates the differences between the four sample surfaces with highlighting the variation in the surface charge.

3.2.2. X-ray photoelectron spectroscopy (XPS)

The sample surfaces were analyzed by XPS. Their spectra of nitrogen (N$_{1s}$), phosphorus (P$_{2p}$), and silicon (Si$_{2p}$) are shown in Fig. 3. The XPS data of atomic concentrations of different sample surfaces are listed in Table 2. Those three MPC copolymers coated substrates were compared with the uncoated substrates. XPS signals at 133 eV attributed to the phosphorus 2p peak and at 402 eV attributed to the nitrogen 1s peak were detected on the PMBASi-, PMSi-, and PMBSSi-coated substrates but not on the uncoated substrates (Fig. 3), revealing the existence of MPC moieties on these coated substrates. On both the PMBSSi- and the PMSi-coated surfaces, the atomic concentrations of nitrogen and phosphorus were almost same, while on the PMBASi-coated surface, the nitrogen concentration was quite higher than the phosphorus concentration due to the trimethylammonium groups of the MTAC moieties on PMBASi (Table 2). The sulfur 2p peak (BE ~ 168 eV) was only detected on the PMBSSi-coated surface, owing to the sulfonate groups of PMPS moieties on PMBSSi. Furthermore, signals at 102 eV attributed to the silicon 2p peak were detected on all samples regardless of whether or not polymer coatings were applied (Fig. 3). However, the atomic concentrations of silicon on the MPC copolymers coated substrates were greatly lower than those on the uncoated substrate (Table 2), suggesting that the substrates were effectively covered by the coating. These results indicate that the substrates were successfully modified by these MPC copolymers.

3.2.3. Surface ζ-potential

The coatings not only changed the surface elemental composition but also altered the surface charge of the original substrate. After coating, the charged moieties of the copolymer played their functions in the form of the interface. The surface ζ-potentials of

sample surfaces were measured to characterize their surface charge in the aqueous environment. As shown in Fig. 4, after coated with the neutral MPC copolymer PMSi, the ζ-potential of the substrate changed from an original value of −47.4 ± 0.9 mV to a value of near 0 mV; the cationic PMBASi-coated substrates and the anionic PMBSSi-coated substrates exhibited ζ-potentials of 26.1 ± 0.6 mV and −24.2 ± 2.5 mV, respectively; the signs of the ζ-potential values were finely in agreement with the variation in the charge properties of the corresponding copolymers; the absolute values of two ζ-potentials of cationic PMBASi and anionic PMBSSi coatings were approximately equal, making them quite comparable. These features indicate that after coating, the charge of the original substrate was shielded, and as a result the polymer layer instead of the surface of the original substrate became to dominate the surface charge condition.

3.2.4. Atomic force microscopy (AFM) and surface roughness

The surface topographies before and after coating were characterized by AFM. The topography images (Fig. 5) demonstrate that all three coated surfaces exhibited as smooth as the uncoated surfaces. The smoothness of sample surfaces was quantitatively verified by analyzing their rms roughness. The uncoated substrate had a very low rms value of 0.43 ± 0.27 nm. The PMBASi-, PMSi-, and PMBASi-coated surface exhibited rms values of 0.36 ± 0.19 nm, 0.15 ± 0.03 nm, and 0.37 ± 0.14 nm, respectively. The rms roughness values of the three coated surfaces were approximate to or lower than that of the uncoated surface, indicating that these coatings did not induce the increase in the surface roughness. Especially, the cationic PMBASi and the anionic PMBSSi-coated surfaces had almost equal rms roughness values, suggesting the type of the charged moiety may not affect the surface roughness.

3.2.5. Surface wettability

To investigate the surface wettability, both the static contact angle (SCA) analysis and the dynamic contact angle (DCA) analysis were performed. The uncoated SiO$_2$ substrate was hydrophilic as it had a 31.2° static contact angle. When a PMSi coating was
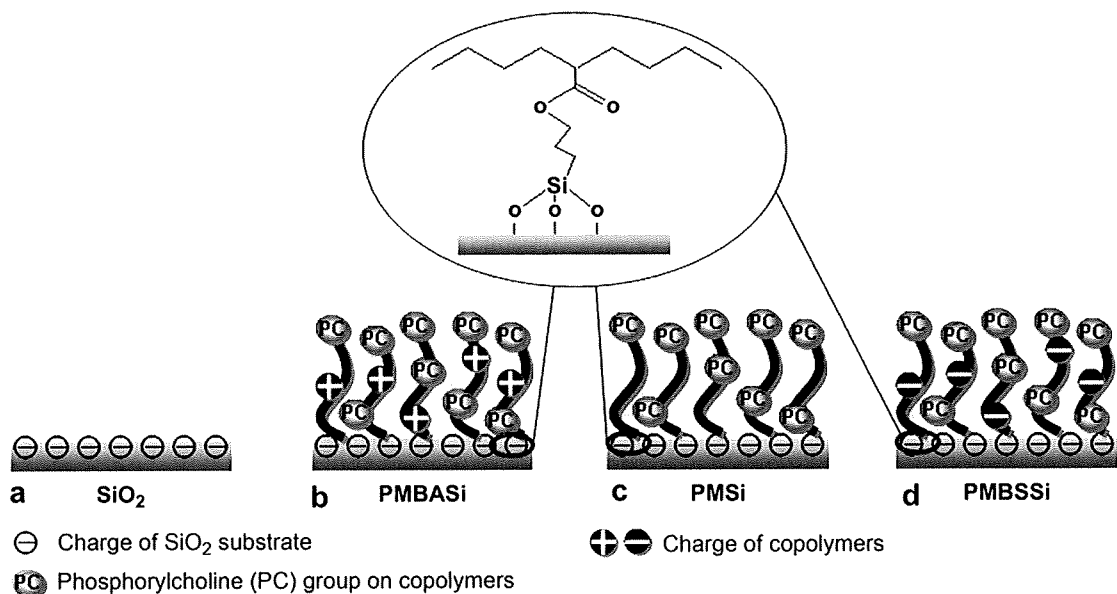

Fig. 2. Sample surfaces used in this study that are prepared using different MPC copolymers and exhibit different surface charges. (a) Uncoated SiO$_2$; (b) PMBASi-coated SiO$_2$; (c) PMSi-coated SiO$_2$; and (d) PMBSSi-coated SiO$_2$. The inset demonstrates the chemical bond between the SiO$_2$ substrate and the MPC polymers.
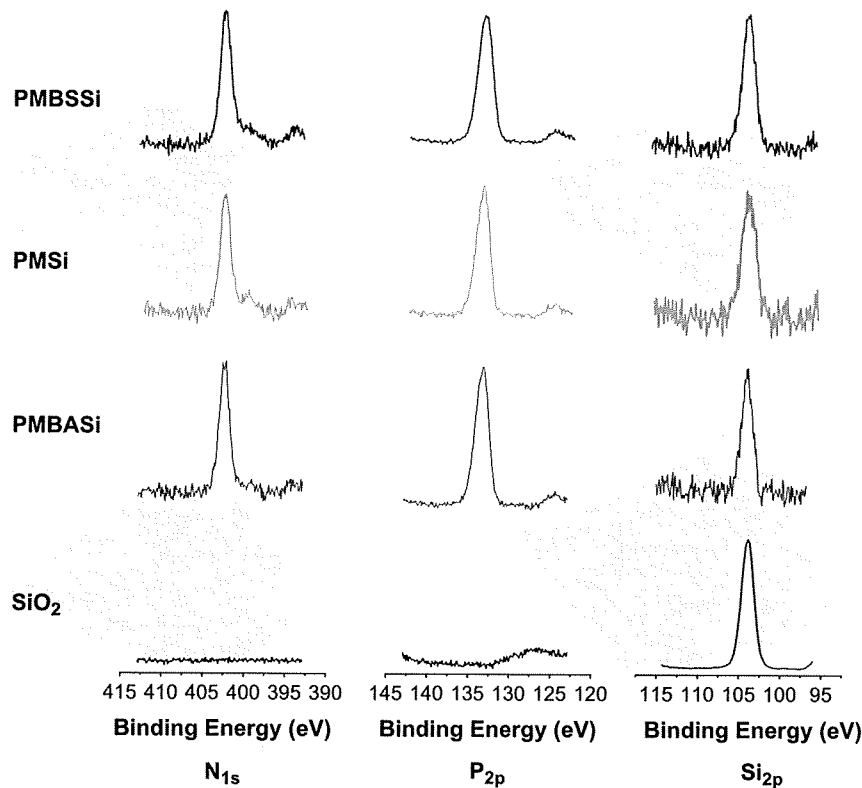
Fig. 3. XPS spectra of nitrogen (N$_{1s}$), phosphorus (P$_{2p}$), and silicon (Si$_{2p}$) on different sample surfaces.

applied, the average contact angle decreased to 10.5°, indicating a highly hydrophilic surface. Both static contact angles of the PMBASi- and the PMBSSi-coated surfaces were lower than that of the uncoated SiO$_2$ surface but higher than that of the PMSi-coated surface. This reveals that, on the one hand both the PMBSASi and the PMBSSi coatings were quite hydrophilic in general, and on the other hand the hydrophobic moieties (i.e., BMA) on both coatings were likely to affect the surface wettability. The role of BMA moieties in the surface wettability was further elucidated by the DCA analysis. The DCA measurement is an easy method to determine the advancing and receding contact angles which are parameters of the surface wettability. The advancing contact angle, θ_A, is sensitive to the hydrophobic surface component, and the receding contact angle, θ_R, is sensitive to the hydrophilic surface component. The DCA profile provides dynamic information on the process from a dry state to a wet state of a surface when in contact with an aqueous medium. Fig. 6 shows the DCA profiles of different sample surfaces. Table 3 summarizes the values of θ_A and θ_R obtained from Fig. 6. As shown in Table 3, in contrast to the PMSi-coated surface, which displayed a low θ_A and a supper low θ_R corresponding to a small hysteresis (Fig. 6), both

the PMBASi- and the PMBSSi-coated surfaces had quite high θ_A and low θ_R, resulting in large hystereses (Fig. 6). Under dry conditions the phosphorylcholine groups of PMBASi and PMBSSi were covered with the hydrophobic moieties of polymer chains to minimize the surface free energy, while the hydrophilic moieties (especially phosphorylcholine groups) became to expose to the aqueous environment to reduce the interfacial energy when contact with water. Hence, the observed large hystereses of PMBASi and PMBSSi may be related to the reorientation of the phosphorylcholine groups when the surface changed from a dry state to a wet state. Through a surface reorientation process, the phosphorylcholine groups would become to dominate the

Table 2
Atomic concentrations of different sample surfaces determined by XPS measurements.

Sample surface	Atomic concentration (%)					
	C$_{1s}$	O$_{1s}$	N$_{1s}$	P$_{2p}$	S$_{2p}$	Si$_{2p}$
SiO$_2$	8.9	60.7	n.d.	n.d.	n.d.	30.4
PMBASi	62.8	28.1	4.5	3.2	n.d.	1.4
PMSi	60.1	28.7	4.8	4.8	n.d.	1.6
PMBSSi	61.9	28.9	3.7	3.8	0.5	1.2

n.d.: not detected.

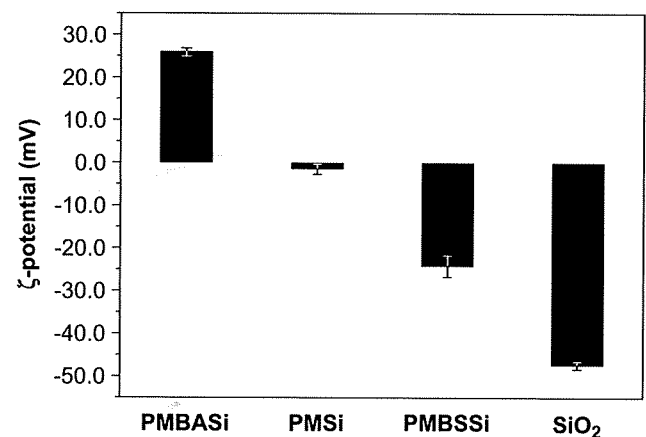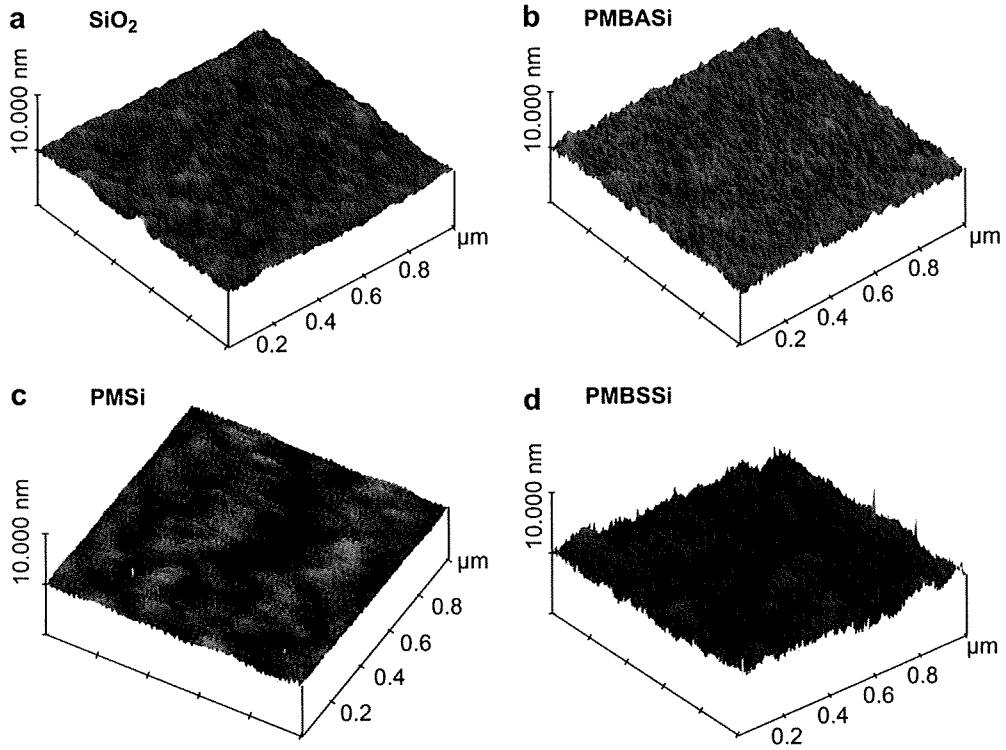**Fig. 4.** Surface ζ-potentials of different sample surfaces. Data are mean ± SD, $n = 6$.

Fig. 5. AFM images (1.0 μm × 1.0 μm areas) of different sample surfaces. (a) Uncoated SiO₂; (b) PMBASi-coated SiO₂; (c) PMSi-coated SiO₂; and (d) PMBSSi-coated SiO₂.
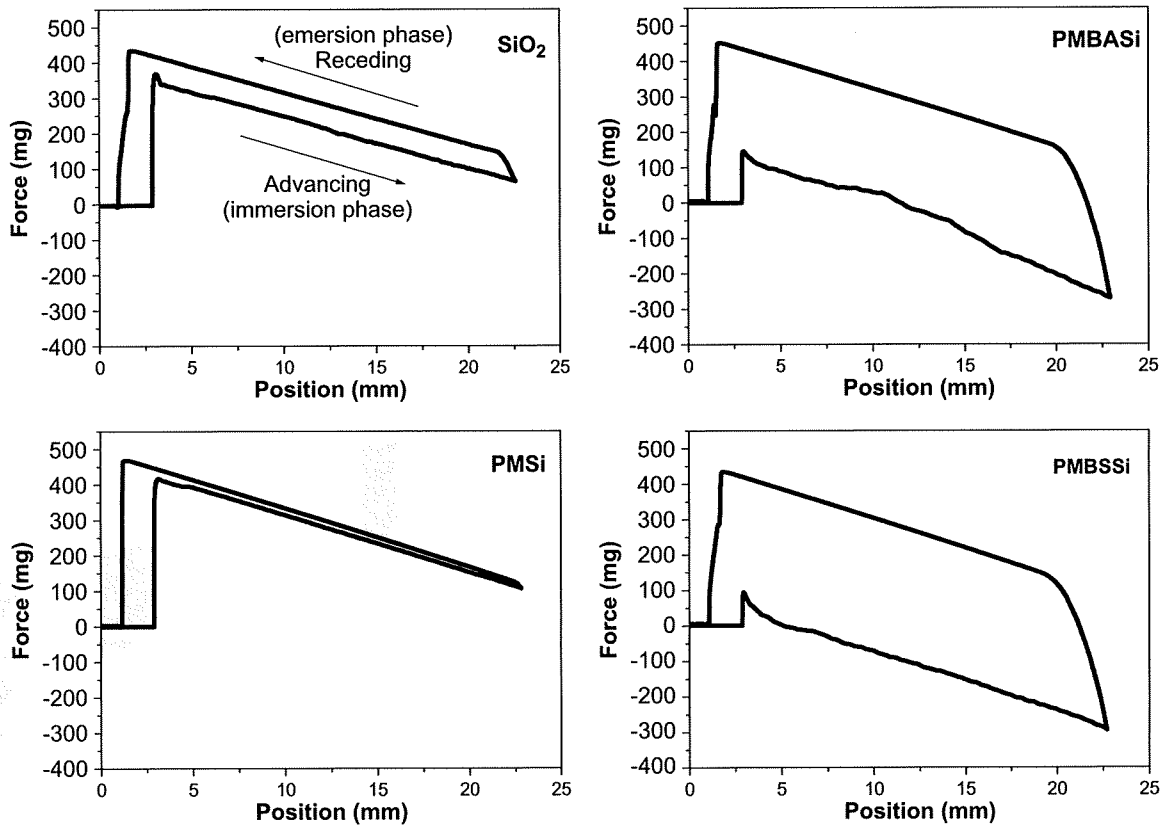

Fig. 6. DCA profiles of different sample surfaces being lowered into ultrapure water at a speed of 80 μm s⁻¹.

Table 3
Advancing and receding contact angles of different sample surfaces.

Sample surface	Contact angle (°)		Hysteresis	Mobility Factor
	Advancing	Receding		
SiO₂	37.1	19.3	17.8	0.48
PMBASi	72.0	11.3	60.7	0.84
PMSi	22.3	0.0	22.3	1.00
PMBSSi	84.4	15.9	68.5	0.81

outmost surface and thereby the hydrophobic moieties would be buried. This is believed very important for an MPC copolymer to play their functions in aqueous mediums [27,28]. According to the value of mobility factor (MF), both the PMBASi- and the PMBSSi-coated surfaces had high mobilities of the polymer chains, implying that when in contact with an aqueous environment, surface reorientation may easily occur in both PMBASi- and PMBSSi-coated surfaces. In addition, a very small hysteresis was observed in the DCA profile of the PMSi-coated surface, which is possibly because phosphorylcholine groups enriched the polymer network and abundantly existed at the surface even under dry conditions [24]. Therefore, the nature of the observed difference in the dynamic wetting process between the PMSi surface and the PMBASi or PMBSSi surface should be ascribed to the introduction of the BMA moieties, which contributed to the hydrophobic surface component and increased the surface hydrophobic/hydrohphlic heterogeneity in the coatings.

3.3. Protein adsorption

The sample surfaces were exposed to a group of proteins to investigate the effects of the surface charge and chemistry on protein adsorption. Based on the electrical nature, we chose pepsin (pI = 1.0) and BSA (pI = 4.7) as typical anionic proteins and ribonuclease A (RNase A, pI = 9.5) and lysozyme (LYZ, pI = 11.0) as typical cationic proteins, respectively. We chose a 1× PBS buffer with a medium ionic strength (about 137 mM) and pH (about 7.1), allowing a better simulation of the typical physiological condition used in various biological applications. Fig. 7 shows the adsorbed amounts of four proteins on uncoated, PMBASi-coated, PMSi-coated, and PMBSSi-coated SiO₂ substrates, determined with a microBCA protocol which is a widely used method to measure trace amount of protein in solution.

The surface coatings remarkably affected the adsorption of the proteins. All proteins, despite their different charge properties, seriously adsorbed to the uncoated SiO₂ substrate, exhibiting high adsorbed amounts. In contrast, the adsorbed protein amounts on three MPC copolymers coated surfaces were pronouncedly low in general. After coating, 82–98% reductions in protein adsorption were obtained in comparison with the corresponding behavior on the uncoated SiO₂ substrates. Generally, a surface with a ζ-potential of about 26.1 mV (ζ-potential of PMBASi) or −24.2 mV (ζ-potential of PMBSSi) can induce protein adsorption significantly. For example, Ikada et al. reported the amounts of BSA adsorption on the different charged monomer grafted
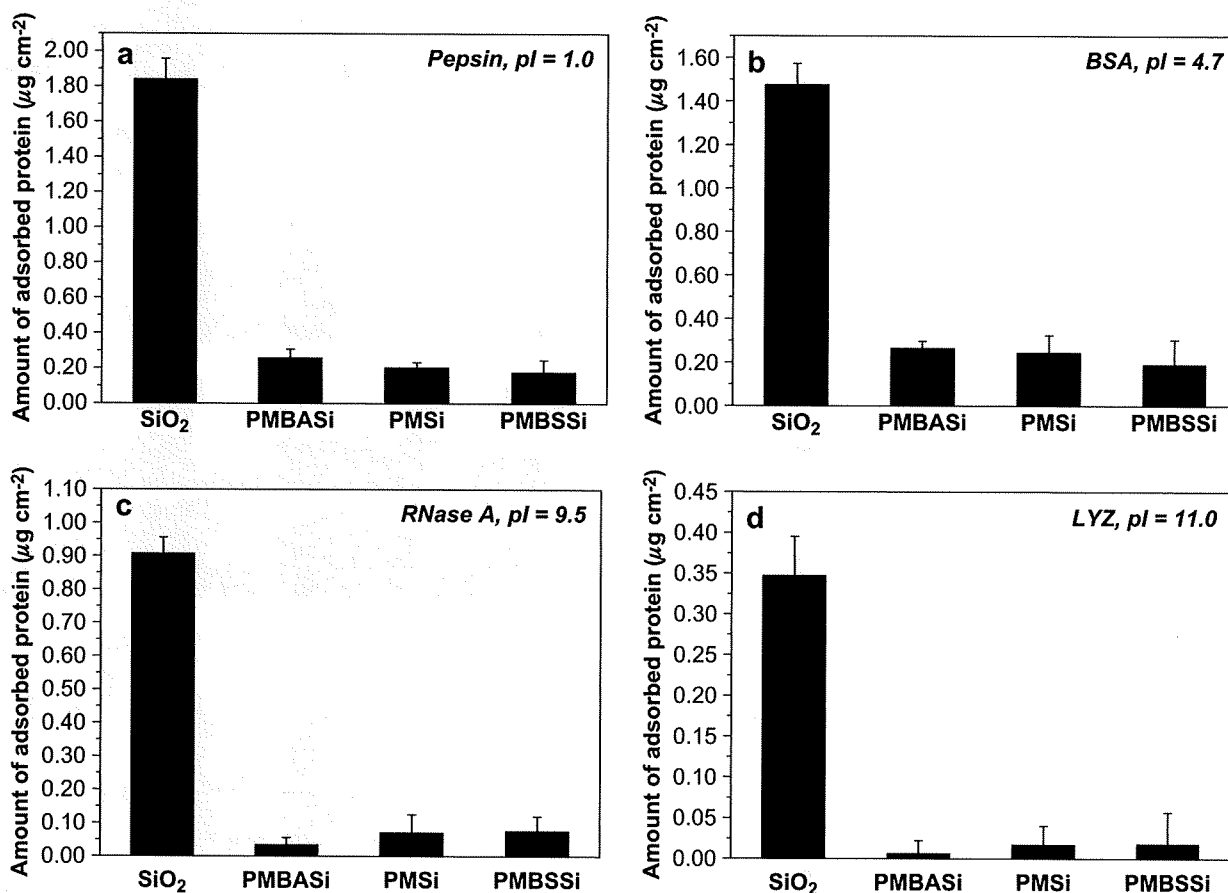
Fig. 7. Amounts of typical cationic proteins and anionic proteins adsorbed on different sample surfaces. (a) pepsin, pI = 1.0; (b) BSA, pI = 4.7; (c) RNase A, pI = 9.5; and (d) LYZ, pI = 11.0.

polyethylene (PE) film surfaces [19]. They carried out the protein adsorption experiments under a similar condition as we used in our experiments. Their results indicated that, the adsorbed amount of BSA on the acrylic acid (AA) grafted PE surface with a ζ-potential of -27.3 mV was 0.78 μg cm^{-2}, an amount which is much higher than that on the PMBSSi surface with a similar ζ-potential; and the adsorbed amount of BSA on the N,N-dimethyl-aminopropyl acrylamide (DMAPAA) grafted PE surface with a ζ-potential of 17.0 mV was 4.76 μg cm^{-2}, an amount which is significantly higher than that on the PMBASi surface with a higher ζ-potential of 26.1 mV. This comparison clearly reveals that despite the charged moieties involved, the MPC moieties on the copolymer still played their role effectively in suppression of protein adsorption. In addition, the adsorbed protein amounts on both the cationic PMBASi surface and the anionic PMBSSi surface were in a similar low level as those on the neutral PMSi surface, with no statistical difference significance. These results indicate that the incorporation of charged moieties would not significantly influence the protein resistant property of an MPC copolymer. Based on previous studies on the effects of ionic strength on protein adsorption, we have made a hypothesis that the function of MPC moieties in the suppression of protein adsorption, rather than the electrostatic character resulting from the charged moieties, dominated the interactions between the protein and the charged MPC copolymer surfaces [11]. The results of this study test, support, and expand the hypothesis.

Considering that the MPC mole fractions in both PMBASi and PMBSSi were only about half of that in PMSi, the fact of no big difference in the protein adsorption on the neutral PMSi surface in comparison with on the charged PMBASi or PMBSSi surfaces implies that, an about 50% mole fraction of the MPC moiety in a copolymer is sufficient to construct a protein adsorption resistant surface and additional more fraction seems not to bring more reduction in the protein adsorption. In addition, as the charged PMBASi and PMBSSi contain hydrophobic moieties (i.e. BMA) but the neutral PMSi dose not, the similar level of protein adsorption meanwhile suggests that the introduction of the hydrophobic moieties in an MPC copolymer surface may not result in an increase in the protein adsorption if the MPC moiety is predominant in the copolymer composition. This should be associated with the fact that both the PMBASi and the PMBSSi surfaces had high mobility as elucidated by the DCA analysis (Fig. 6 and Table 3). The high mobility facilitates the surface reorientation when the surface is in contact with an aqueous medium, and the hydrophobic components (for example, BMA in both PMBASi and PMBSSi) are buried in the inner of the polymer layer as the hydrophilic components such as MPC moieties migrate to the outmost surface to minimize the surface energy [27,28]. The MPC moieties are predominant at the surface and thereby dominate the surface properties, especially such as the interactions with proteins when in contact with a protein solution.

Although the adsorbed protein amounts on three coated surfaces had no statistical difference significance with each other, quantitatively they still present a subtle but systematic dependence on the surface charge. When ranking the amounts of protein adsorbed on the different coated surfaces, in the cases of negatively charged pepsin and BSA (Fig. 7a and b), the order is PMBASi (cationic) > PMSi (neutral) > PMBSSi (anionic), while in the cases of positively charged RNase A and LYZ (Fig. 7c and d), the order is PMBASi (cationic) < PMSi (neutral) < PMBSSi (anionic). This can be correlated to the possible electrostatic interactions between the charged proteins and the charged surfaces [17]. However, as discussed above, the possible effect from electrostatic interactions would be too small and too limited to influence the overall situation.

3.4. Cell adhesion

At the molecular level, it is generally believed that the rapid adsorption of proteins to the surface is the initial stage of cell adhesion [29]. In view of the high capability of the three MPC copolymers to suppress protein adsorption, we supposed that they would have corresponding capability to resist the cell adhesion. Mouse fibroblast L929 cells, which are typical adherent cells and are widely used in various biological studies and evaluations as model cells, were employed to evaluate the cell adhesion on the sample surfaces. Fig. 8 shows the microscopic images of sample surfaces on which L929 cells were cultured for one day and four days. In the case of uncoated surface, L929 cells gradually adhered,
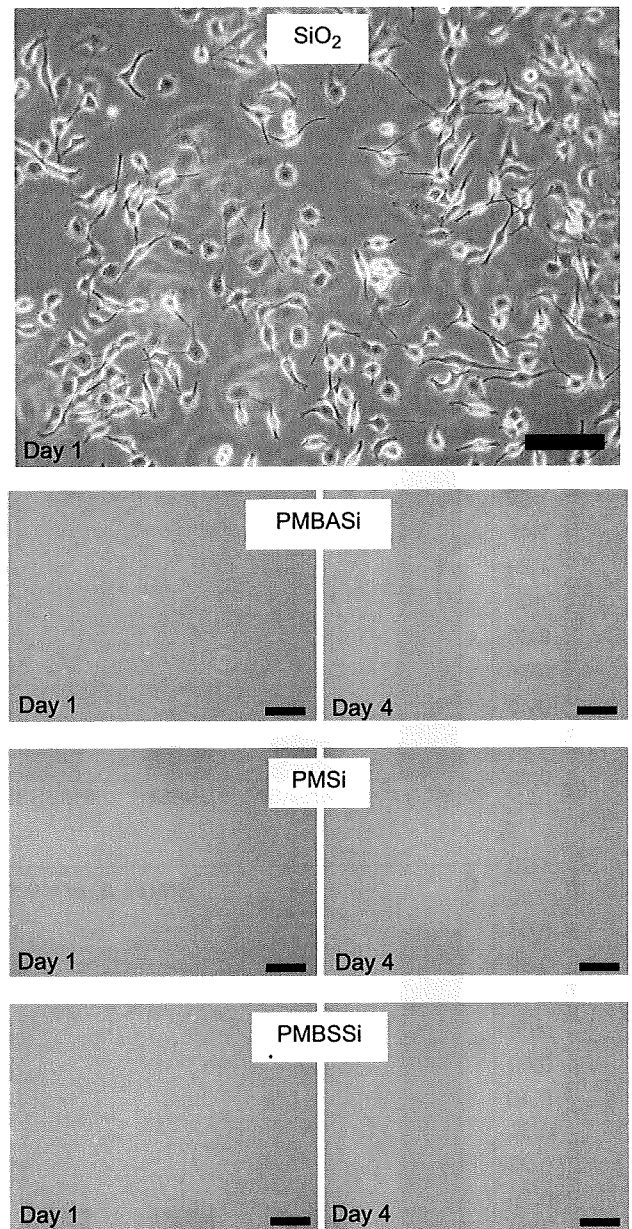

Fig. 8. Microscopic images of different sample surfaces on which L929 cells were cultured for one day and four days. MPC copolymers coated SiO$_2$ surfaces exhibited no cell adhesion, while uncoated SiO$_2$ exhibited serious cell adhesion. Scale bar represents 100 μm.

spread, and flattened on the surface after seeded, and then formed confluence after cultured for one day (Fig. 8), and finally densely covered the surface four days later (data not shown). In contrast, no cell adhesion was observed on PMBASi, PMSi, and PMBSSi surfaces after cultured for one day and even for four days (Fig. 8). This indicates that like the neutral PMSi, both the cationic PMBASi and the anionic PMBSSi possess the high capability to suppress cell adhesion due to the MPC moieties at the surface. Ikada et al. reported that cells could adhere and proliferate on the charged monomer grafted PE surfaces with a ζ-potential larger than 12 mV [19]. Before we performed the evaluation, we had previously speculated that the cationic PMBASi surface might induce cell adhesion because of the possibly increased electrostatic attraction between the positive charged surface of the coating and the negatively charged surface of the cell. Evidently, the evaluation result overturned the speculation, and it seems that the charged moieties in PMBASi and PMBSSi would not cause the effect in inducing cell adhesion. This further supports our aforementioned hypothesis that the electrostatic character resulting from the charged moieties of the copolymers would not dominate the surface behaviors of bioadsorptions.

4. Conclusions

The behaviors of protein adsorption and cell adhesion on three model MPC copolymer surfaces with different surface charges were comparatively investigated. Results imply that the introduction of charged moieties, either the cationic or the anionic, in an MPC copolymer, would not increase the risk in inducing both the protein adsorption and cell adhesion. This tests, supports, and expands our previous hypothesis that the function of MPC moieties in the suppression of protein adsorption, rather than the electrostatic character resulting from the charged moieties, would dominate the interactions between proteins/cells and MPC copolymer surfaces. These electrically charged MPC copolymer surfaces can be applied to those biological applications simultaneously requiring non-biofouling properties and electrical properties.

Acknowledgement

Appendix

Figures with essential colour discrimination. Certain figures in this article, in particular Figures 2, 3, 5 and 8, are difficult to interpret in black and white. The full colour images can be found in the on-line version, at doi:10.1016/j.biomaterials.2009.06.005.

References

[1] Ishihara K, Ueda T, Nakabayashi N. Preparation of phospholipid polymers and their properties as polymer hydrogel membranes. Polym J 1990;22:355–60.

[2] Ishihara K, Nomura H, Mihara T, Kurita K, Iwasaki Y, Nakabayashi N. Why do phospholipid polymers reduce protein adsorption? J Biomed Mater Res 1998;39:323–30.

[3] Iwasaki Y, Ishihara K. Phosphorylcholine-containing polymers for biomedical applications. Anal Bioanal Chem 2005;381:534–46.

[4] Palmer RR, Lewis AL, Kirkwood LC, Rose SF, Lloyd AW, Vick TA, et al. Biological evaluation and drug delivery application of cationically modified phospholipid polymers. Biomaterials 2004;25:4785–96.

[5] Chim YTA, Lam JKW, Ma Y, Armes SP, Lewis AL, Roberts CJ, et al. Structural study of DNA condensation induced by novel phosphorylcholine-based copolymers for gene delivery and relevance to DNA protection. Langmiur 2005;21:3591–8.

[6] Chiba N, Ueda M, Shimada T, Jinno H, Watanabe J, Ishihara K, et al. Development of gene vectors for pinpoint targeting to human hepatocytes by cationically modified polymer complexes. Eur Surg Res 2007;39:23–32.

[7] Zhao XB, Pan F, Coffey P, Lu HR. Cationic copolymer-mediated DNA immobilization: interfacial structure and composition as determined by ellipsometry, dual polarization interferometry, and neutron reflection. Langmuir 2008; 24:6881–8.

[8] Morille M, Passirani C, Vonarbourg A, Clavreul A, Benoit JP. Progress in developing cationic vectors for non-viral systemic gene therapy against cancer. Biomaterials 2008;29:3477–96.

[9] Allen TM, Cullis PR. Drug delivery systems: entering the mainstream. Science 2004;303:1818–22.

[10] Xu Y, Takai M, Konno T, Ishihara K. Microfluidic flow control on charged phospholipid polymer interface. Lab Chip 2007;7:199–206.

[11] Xu Y, Takai M, Ishihara K. Suppression of protein adsorption on a charged phospholipid polymer interface. Biomacromolecules 2009;10:267–74.

[12] Ge XW, Ye Q, Xu XL, Zhang ZC, Chu GS. Studies of inverse emulsion copolymerization of (2-methacryloyloxyethyl) trimethyl ammonium chloride and acrylamide. J Appl Polym Sci 1998;67:1005–10.

[13] Hou SJ, Ha RH. The electrochemical analysis of cationic water soluble polymer. Eur Polym J 1998;34:283–6.

[14] Roach P, Farrar D, Perry CC. Surface tailoring for controlled protein adsorption: effect of topography at the nanometer scale and chemistry. J Am Chem Soc 2006;128:3939–45.

[15] Mrksich M. A surface chemistry approach to studying cell adhesion. Chem Soc Rev 2000;29:267–74.

[16] Ostuni E, Yan L, Whitesides GM. The interaction of proteins and cells with self-assembled monolayers of alkanethiolates on gold and silver. Colloid Surf B Biointerfaces 1999;15:3–30.

[17] Pasche S, Voros J, Griesser HJ, Textor M. Effects of ionic strength and surface charge on protein adsorption at PEGylated surfaces. J Phys Chem B 2005;109:17545–52.

[18] Ladd J, Zhang Z, Chen S, Hower JC, Jiang S. Zwitterionic polymers exhibiting high resistance to nonspecific protein adsorption from human serum and plasma. Biomacromolecules 2008;9:1357–61.

[19] Kishida A, Iwata H, Tamada Y, Ikada Y. Cell behavior on polymer surfaces grafted with nonionic and ionic monomers. Biomaterials 1991;12:786–92.

[20] Rechendorff K, Hovgaard MB, Foss M, Zhdanov VP, Besenbacher F. Enhancement of protein adsorption induced by surface roughness. Langmuir 2006;22:10855–88.

[21] Anselme K, Bigerelle M, Noel B, Dufresne E, Judas D, Iost A, et al. Qualitative and quantitative study of human osteoblast adhesion on materials with various surface roughnesses. J Biomed Mater Res 2000;49:155–66.

[22] Sethuraman A, Han M, Kane RS, Belfort G. Effect of surface wettability on the adhesion of proteins. Langmuir 2004;20:7779–88.

[23] Arima Y, Iwata H. Effect of wettability and surface functional groups on protein adsorption and cell adhesion using well-defined mixed self-assembled monolayers. Biomaterial 2007;28:3074–82.

[24] Futamura K, Matsuno R, Konno T, Takai M, Ishihara K. Rapid development of hydrophilicity and protein adsorption resistance by polymer surfaces bearing phosphorylcholine and naphthalene groups. Langmuir 2008;24:10340–4.

[25] Jang K, Sato K, Mawatari K, Konno T, Ishihara K, Kitamori T. Surface modification by 2-methacryloyloxyethyl phosphorylcholine coupled to a photolabile linker for cell micropatterning. Biomaterials 2009;30:1413–20.

[26] Lewis AL, Cumming ZL, Goreish HH, Kirkwood LC, Tolhurst LA, Stratford PW. Crosslinkable coatings from phosphorylcholine-based polymers. Biomaterials 2001;22:99–111.

[27] Clarke S, Davies MC, Roberts CJ, Tendler SJB, Williams PM, O'Byrne V, et al. Surface mobility of 2-methacryloyloxyethyl phosphorylcholine-co-lauryl methacrylate polymers. Langmuir 2009;16:5116–22.

[28] Feng W, Zhu SP, Ishihara K, Brash JL. Adsorption of fibrinogen and lysozyme on silicon grafted with poly(2-methacryloyloxyethyl phosphorylcholine) via surface-initiated atom transfer radical polymerization. Langmuir 2005; 21:5980–7.

[29] Ostuni E, Chapman RG, Liang MN, Meluleni G, Pier G, Ingber DE, et al. Self-assembled monolayers that resist the adsorption of proteins and the adhesion of bacterial and mammalian cells. Langmuir 2001;17:6336–43.

ELSEVIER
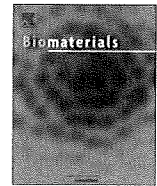
Cell adhesion on phase-separated surface of block copolymer composed of poly-(2-methacryloyloxyethyl phosphorylcholine) and poly(dimethylsiloxane)

Ji-Hun Seo [a,c], Ryosuke Matsuno [a,c], Madoka Takai [a,c], Kazuhiko Ishihara [a,b,c,*]

[a] Department of Materials Engineering, School of Engineering, The University of Tokyo, 7-3-1 Hongo, Bunkyo-ku, Tokyo 113-8656, Japan
[b] Department of Bioengineering, School of Engineering, The University of Tokyo, 7-3-1 Hongo, Bunkyo-ku, Tokyo 113-8656, Japan
[c] Center for NanoBio Integration, The University of Tokyo, 7-3-1 Hongo, Bunkyo-ku, Tokyo 113-8656, Japan

ARTICLE INFO

ABSTRACT

We investigated the morphological effect of phase-separated block copolymer surfaces composed of poly(2-methacryloyloxyethyl phosphorylcholine (MPC)) (PMPC) and poly(dimethylsiloxane) (PDMS) on protein adsorption and cell adhesion behavior. We observed three different types of phase-separated surface morphologies by TEM and AFM. The elemental composition of phosphorus on the surface increases with the PMPC composition. Furthermore, the polymer surface formed by a block copolymer-containing a higher MPC unit composition shows a slightly lower static water contact angle. This result indicates that the elemental surface ratio of the surface depends on the MPC composition in the block copolymer. Protein adsorption tests revealed that only hydrophobic PDMS domains showed selective protein adsorption. Cell adhesion tests revealed that the number of adhered cells increased with increasing hydrophobic PDMS domain size of block copolymers in serum-containing media. In contrast, no cells adhered onto block copolymer surfaces in serum-free media, whereas a large amount of adhered cells were observed on the hydrophobic PDMS surface. This result indicates that segregated hydrophobic domains on a biocompatible PMPC surface strongly affect serum protein adsorption, thereby promoting considerable cell adhesion, although the surface is hydrophilic. Thus, both the composition of MPC units and the segregated hydrophobic surface morphology are important considerations in biomaterial surface design.

© 2009 Elsevier Ltd. All rights reserved.

1. Introduction

It is well known that significant plasma protein adsorption initially occurs on artificial material surfaces in biological environments. Such adsorbed proteins are believed to mediate cell adhesion and activation, thus promoting platelet adhesion and even thrombosis [1], which are principal drawbacks to medical applications of artificial biomaterials. For that reason, investigation of surface-induced effects of polymer materials, such as roughness and hydrophilicity, on plasma protein adsorption and, ultimately, on cellular adhesion behavior has been a key area of biomaterial research. Over the past few years, several research groups have studied the quantitative relationship between cellular adhesion and surface adsorption of serum proteins [2]. These studies reported that even very low concentrations of cell adhesive serum proteins, such as fibrinogen or von Willebrand's factor adsorbed on hydrophilic

material surface, have almost the same effect on platelet adhesion with those of adsorption levels on hydrophobic surfaces [3].

Recently, in addition to the quantitative relationships described above, the spatial relationship of heterogeneous material surfaces and serum protein adsorption has become a matter of concern in investigations of cellular responses on material surfaces. Sousa et al. reported that heterogeneous polymer domains obtained by phase separation of polymer blends induce preferential adsorption behavior of serum proteins [4]. Another study showed that heterogeneous morphologies developed by different monomer compositions of block copolymers had different cell adhesion morphologies with regard to serum proteins [5]. More recently, Arnold et al. reported that only a single cell-adhesive peptide, spatially existing on a poly(ethylene glycol) (PEG) passivated surface, influences cell adhesion behavior [6]. Although several important factors, such as roughness or stiffness of the materials surface, must be considered in order to gain an integral understanding of cellular interactions on surfaces, it is now clear that even a small amount of cell-adhesive serum proteins on heterogeneous material surfaces must be a primary consideration when designing any biomaterial.

---

* Corresponding author. Department of Materials Engineering, The University of Tokyo, 7-3-1 Hongo, Bunkyo-ku, Tokyo 113-8656, Japan. Tel.: +81 3 5841 7124; fax: +81 3 5841 8647.
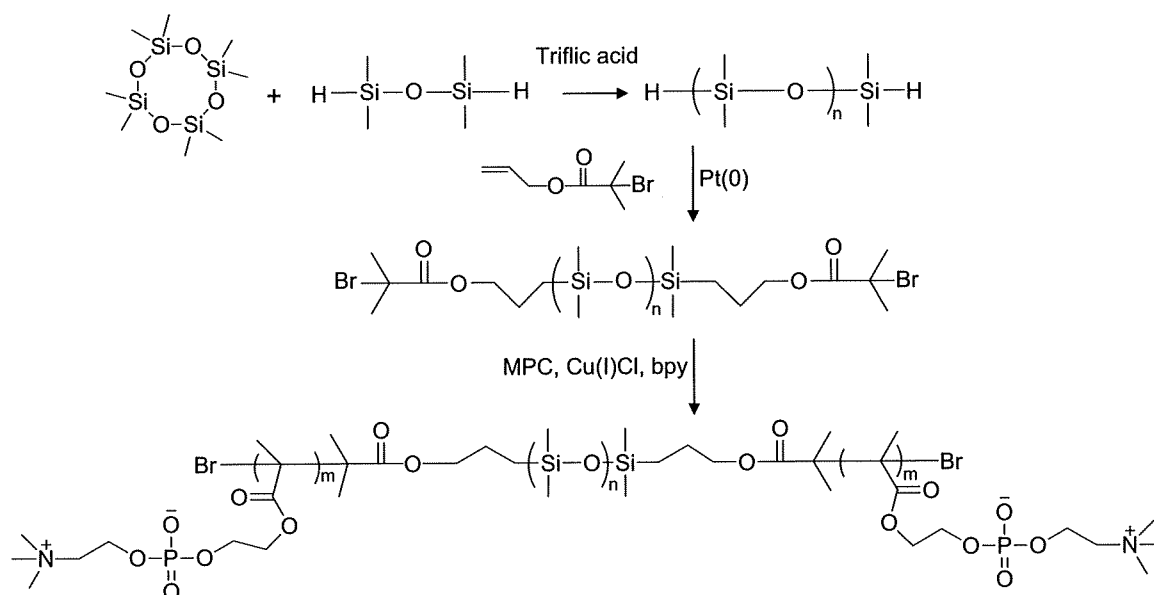E-mail address: ishihara@mpc.t.u-tokyo.ac.jp (K. Ishihara).

Scheme 1. Synthetic route and molecular structure of block copolymer.

Table 1
Characterization of synthesizes PDMS and block copolymers.

	Monomer unit composition (%, NMR)		Molecular weight (M_n, kDa)		Polydispersity index (PDI)
	MPC	PDMS	GPC	NMR	
PDMS1	–	–	1.02	–	1.44
PDMS2	–	–	4.21	–	1.90
PDMS3	–	–	7.96	–	1.51
PM1	88.0	12.0	36.7	31.9	1.27
PM2	59.3	40.7	56.7	28.3	1.35
PM3	44.6	55.4	34.2	31.7	1.43

2-Methacryloyloxytheyl phosphorylcholine (MPC) is a very well known biomaterial that exhibits excellent blood compatibility and biocompatibility by suppression of cellular responses on its surface [7–12]. Because the phosphorylcholine group possesses a large amount of free water, serum proteins can contact the MPC polymer surface in a reversible manner [13]. For that reason, many biomedical interfaces containing MPC polymers have been successfully developed by a wide range of materials preparation methods, such as random copolymerization of MPC with other alkyl methacrylates or surface grafting from various substrates [14–17]. As a result, homogeneously prepared material surfaces derived from MPC polymers have shown excellent antibiofouling and antithrombosis properties, even when they were in contact with whole blood [18].

In addition to homogeneously prepared biomaterials, MPC polymer-containing binary materials, such as polymer blends or block copolymers, have also been introduced for the development of biomedical applications [19–22]. These materials have distinctive physical properties, including flexibility and formability. Thus, a MPC polymer-containing binary material has found application as a safe blood contact material, with use as an artificial blood vessel [23].
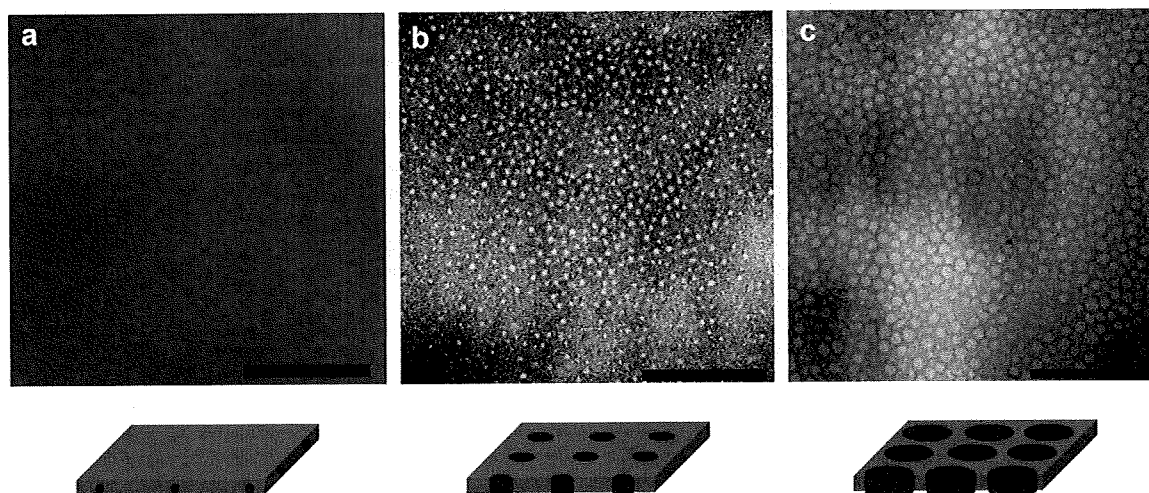

Fig. 1. Bright-field TEM images of block copolymers (a) PM1, (b) PM2, and (c) PM3 taken after staining with OsO4. The dark region indicates OsO4 stained PMPC domains and bright region indicates segregated PDMS domains. Scale bar = 300 nm. Red and blue region in the scheme indicate the PMPC and PDMS domains, respectively.
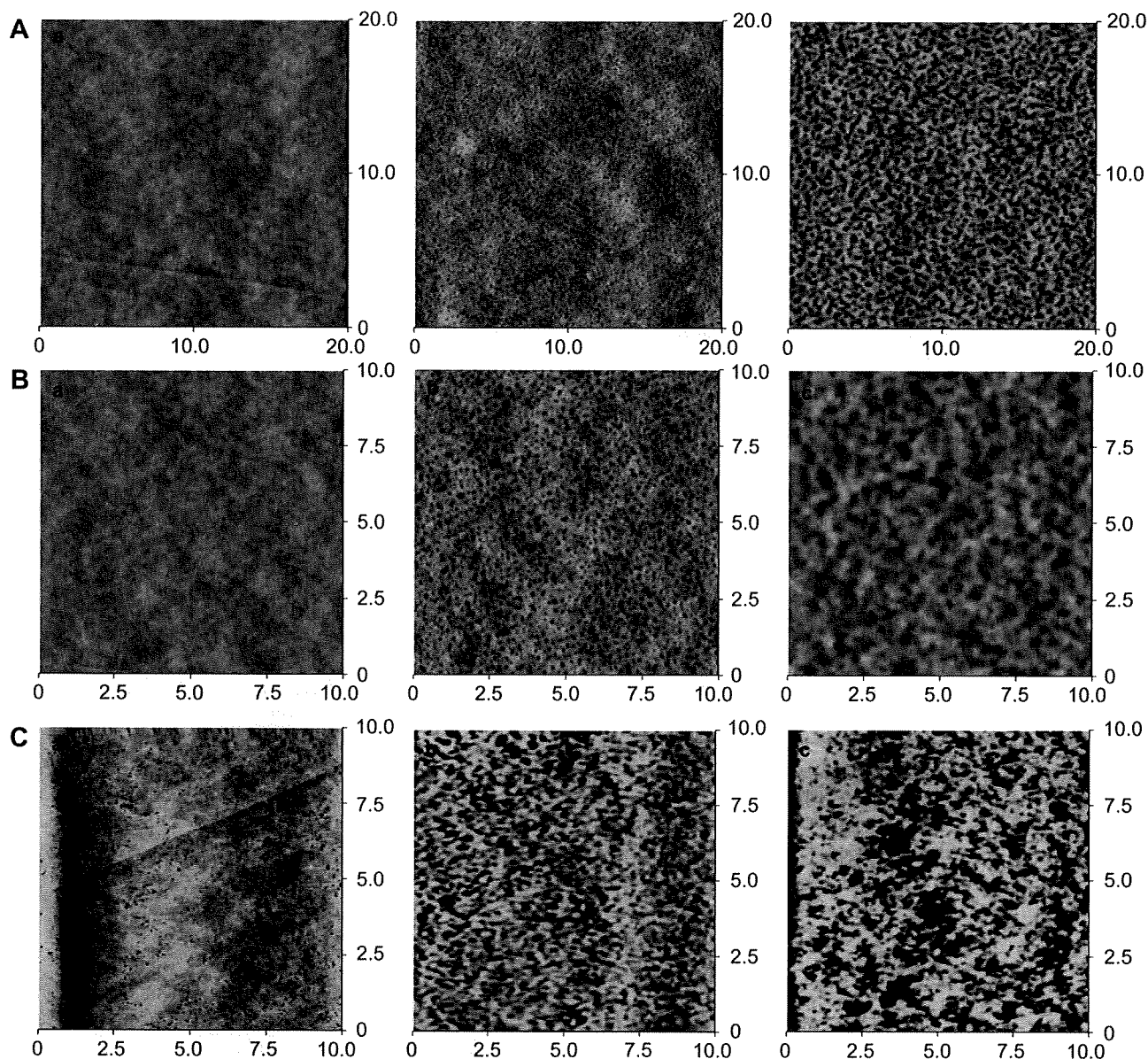
Fig. 2. A. AFM topological images of (a) PM1, (b) PM2, and (c) PM3 under dry conditions with 20 μm × 20 μm scan size. B. AFM topological images of (a) PM1, (b) PM2, and (c) PM3 under dry conditions with 10 μm × 10 μm scan size. C. AFM topological images of (a) PM1, (b) PM2, and (c) PM3 taken in PBS with 10 μm × 10 μm scan size.

Although these binary materials have been effective in suppressing thrombus formation or protein adsorption, their surface morphological effects have not been studied extensively. Because contact between each component in these binary materials is unfavorable from an enthalpy standpoint, heterogeneous morphologies induced by phase separation are inevitable in such binary material systems [24]. For that reason, interactions between heterogeneous MPC polymer surfaces and plasma proteins, which could promote cell adhesion behavior as above-mentioned references, have to be investigated for defining cellular responses on MPC polymer-containing binary materials surfaces.

In our current study, we examine the surface morphological effect of a heterogeneous MPC polymer on protein adsorption and cell adhesion behavior under existence of serum proteins. In order to investigate the size effect of segregated hydrophobic domains, we prepared three different compositions of ABA type triblock copolymers composed of poly(MPC) (PMPC) and

poly(dimethylsiloxane) (PDMS) by the atom transfer radical polymerization (ATRP) method. As a result, three kinds of heterogeneous MPC polymer surfaces having different hydrophobic domain size were prepared by solvent cast method. Because PDMS is a very well known hydrophobic material that induces significant protein adsorption and cell adhesion on its surface, we expected heterogeneous surfaces developed from block copolymers to contain both biofouling and antibiofouling domains. We focus in this work on the effect of selective hydrophobic interactions between proteins and PDMS domains and the resulting cell adhesion behavior.

2. Materials and methods

2.1. Materials

MPC was synthesized by a previously reported method [25]. Octamethyl-cyclotetrasiloxane (D_4), 1,1,3,3-tetramethyldisiloxane (TMS), and trifluoromethane-sulfonic acid (triflic acid) were purchased from Tokyo Chemical Industry Co., Ltd.

(Tokyo, Japan). Allyl 2-bromoisobutylate, Cu(I)Cl, 2,2′-bipyridyl, 10 nm diameters of gold colloid-labeled immunoglobulin G (IgG, whole molecules from goat), non-labeled IgG, fibronectin (from bovine plasma), and Karstedt's catalyst were purchased from Sigma–Aldrich (St. Louis, MO, USA). 2-Methyl-1,4-naph-thoquinone, Triton X-100, 4′,6-diamidino-2-phenylindole dihydrochloride (DAPI), and all organic solvents (organic synthesis grade) were purchased from Wako Chemical Co. (Osaka, Japan) and used as-received. Dulbecco's phosphate buffered saline (×10) (PBS; pH 7.4, without calcium chloride and magnesium chloride), Alexa Fluor 488 phalloidin was purchased from Invitrogen Co. (Carlsbad, CA, USA). A micro-BCA™ protein assay reagent kit (#23235) was purchased from Pierce Chemical (Rockford, IL, USA) and a Cell Counting Kit-8 was purchased from Dojindo Laboratories Co. (Tokyo, Japan).

2.2. Synthesis of silylhydrated end functional PDMS

The representative synthesis process for hydrosilyl-terminated PDMS is as follows. 20 g of D_4 (0.068 mol) and 0.24 mL of 1,1,3,3-tetramethyldisiloxane (1.36 mmol) were placed in a round-bottomed flask, degassed by Ar bubbling for 10 min, and then sealed right after 0.13 mL of triflic acid was injected. The mixture was placed in a 55 °C oil bath for 3 days. Next, the white mixture was dissolved in ether and repeatedly washed with water until it was neutralized. The ether was isolated and stirred overnight with magnesium sulfate following filtration and vacuum treatment at 120 °C for 1 day. Three different molecular weights of PDMS were synthesized by controlling D_4/TMS ratios. Synthesis of PDMS macroinitiators and ATRP with MPC was carried out by means of a previously reported method [26]. The overall reaction scheme is illustrated in Scheme 1.

2.3. Preparation of block copolymer substrate

One weight percent of each block copolymer solution in ethanol was cast on poly(ethyleneterephthalate) (PET) substrate and naturally dried. Next, the substrates were heat treated at 60 °C under reduced pressure for 3 days. For the cell adhesion test, the same process was carried out in a 24-well tissue culture poly(styrene) (TCPS) dish followed by ultraviolet treatment to ensure sterilization.

2.4. Surface characterization

2.4.1. Morphological analysis of block copolymer surface

Block copolymers were cast on a copper grid (grid pitch 100 μm, carbon membrane supported) for observation by transmission electron microscopy (TEM). Cast membrane was then heat treated at 60 °C for 3 days *in vacuo*. For observation of protein adsorption behavior, commercial 10-nm gold colloid-labeled IgG solution was diluted one-third in phosphate buffered saline (PBS, pH 7.4), and placed in contact with a casting grid for 10 min at room temperature. After thorough washing with fresh PBS, the grid was dried under reduced pressure for 1 day and stained with 2% osmium (VIII) oxide solution (Wako Chemical, Osaka, Japan) by a dry staining method, after which TEM (Hitachi H-800, acceleration voltage: 100 kV, Tokyo, Japan) studies were conducted. Topological analyses of block copolymer templates were performed using atomic force microscopy (AFM; Nihon Veeco, Nanoscope IIIa, Tokyo, Japan). The excitation frequency range was 7.8–9.0 kHz, and the scan rate and scan scales were 0.5 Hz and 5 nm, respectively, with 20 μm × 20 μm scan sizes.
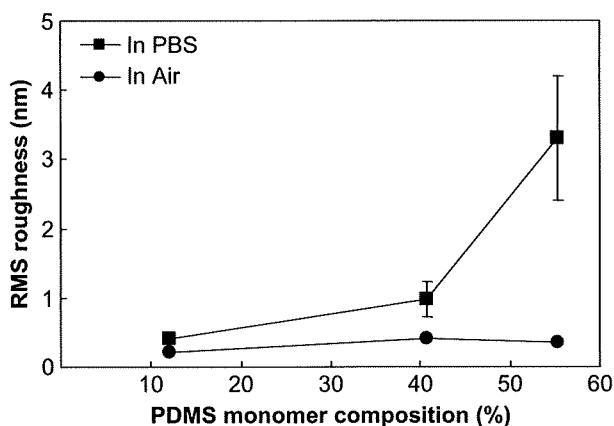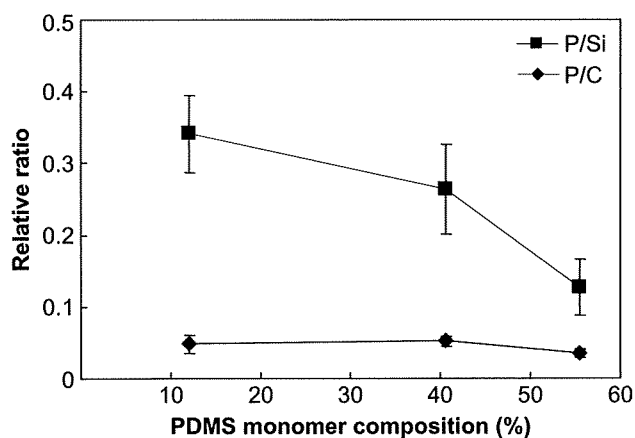
Fig. 4. P/C and P/Si values of block copolymer surfaces calculated by XPS analysis as a function of PDMS compositions. Each point indicates PM1, PM2, and PM3 from left to right.

Atomic force microscopy (AFM) under wet conditions was performed in PBS at room temperature after equilibration in PBS at 37 °C for 1 h.

2.4.2. Surface characterization

Static water contact angles of the block copolymer surface were measured by using a goniometer (Kyowa Interface Science Co., Tokyo, Japan). 3 μL of water droplets were brought into contact with each sample for 10 s, and the contact angles were measured and recorded as photographic images. Elemental analyses of surfaces were performed by X-ray photoelectron spectroscopy (XPS) measurement (Kratos/Shimadzu, Kyoto, Japan), using magnesium Kα sources with 90° of photoelectron takeoff angle. Elements characterized included C, N, P, and Si. Binding energies were referenced to the C1s peak at 285.0 eV. P/C and P/Si values were calculated by integration of each peak area.

2.5. Biological responses on the block copolymer surfaces

2.5.1. Proteins adsorption test

Block copolymer templates were prepared in 24-well plates (TCPS) for the protein adsorption test. 1 mL of IgG or fibronectin solution (0.45 mg/mL in PBS, pH 7.4) was poured into each well and incubated at 37 °C for 1 h. Next, the protein solutions were removed, and the wells were carefully washed with fresh PBS twice. After adding 0.5 mL of sodium dodecyl sulfate (SDS) (10 mg/mL), each plate was sonicated for 20 min at room temperature. Protein concentration in SDS solution was then determined using a micro-BCA™ protein assay reagent kit.

2.5.2. Cell adhesion test

A cell adhesion test using L929 mouse fibroblast cells (RCB 0081, Cell Bank, Japan) on block copolymers was performed in 24-well plates. Approximately 3.0×10^4 cells were grown in 1 mL of minimum essential medium (Invitrogen Co.

Fig. 3. Root mean square (RMS) value of surface roughness of block copolymer surfaces in PBS and under dry conditions as a function of PDMS compositions. Each point indicates PM1, PM2, and PM3 from left to right.
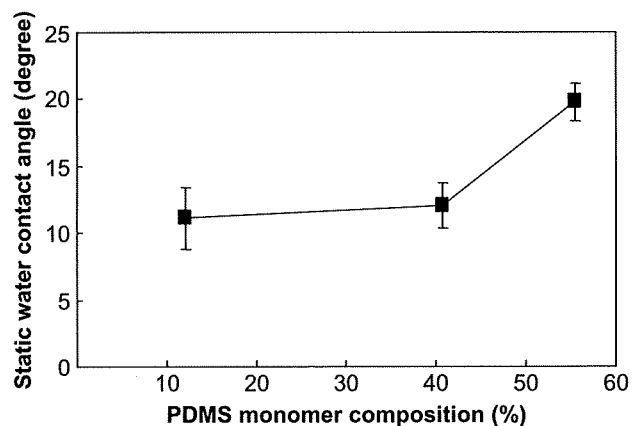
Fig. 5. Static contact angles of block copolymers as a function of PDMS compositions.
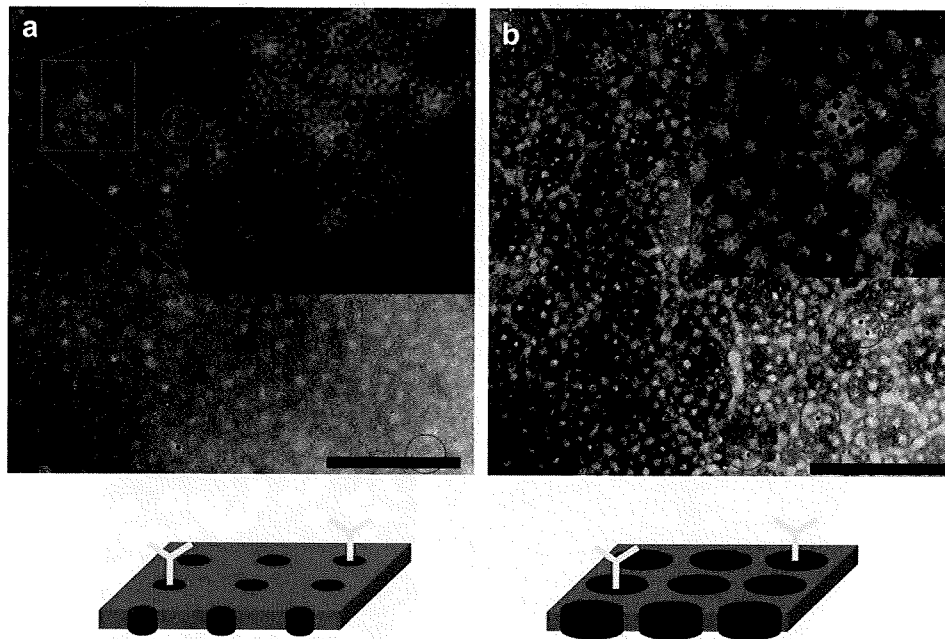
Fig. 6. Bright-field TEM images of block copolymer surfaces taken after contact with Au colloid-labeled IgG solution; (a) PM2 and (b) PM3. Small dark dots indicate Au colloid-labeled IgG molecules. Scale bar = 300 nm. The size of enlarged part is 170 nm × 170 nm and 200 nm × 200 nm, respectively. Red and blue region in the scheme indicate the PMPC and PDMS domains, respectively.

Carlsbad, CA, USA), supplemented (or not) by 10% fetal bovine serum (FBS). Plates were incubated in a 100% humidified incubator at 37 °C with 5% CO_2 for a maximum of 4 days. Cell morphologies were observed by using an optical microscope (Olympus Optical Co. LTD. IX71S1F-2, Tokyo, Japan). For fluorescent microscopic observation, cells on block copolymer templates were stained as follows: Each well was carefully washed with fresh PBS and fixed with 4.0% of paraformaldehyde for 10 min at room temperatures. After washing with fresh PBS, cells were permeabilized with 2.5% Triton X-100 for 10 min and rinsed again with PBS. Alexa Fluo 488 phalloidin (diluted 1:200) was then added, and the cells were incubated in the dark for 45 min at room temperature. After rinsing with fresh PBS, 1:1000 diluted DAPI solution (PBS, pH 7.4) was added, and the cells were incubated for another 15 min at room temperature. Next, the wells were washed with PBS, and block copolymer surfaces were kept in a wet condition with fresh PBS for the confocal laser microscopic observation (LSM 510, Carl Zeiss Japan, Tokyo, Japan). Number of cells was calculated by injecting 1/10 volume of Cell Counting Kit #8 into each well, followed by incubation at 37 °C for 2 h, using self-made calibration data.

3. Results and discussion

3.1. Synthesis of end functional PDMS

Surface morphology of a block copolymer induced by phase separation is dominated by several physicochemical factors, including solubility, composition, degree of polymerization, and molecular weight [24]. In order to minimize other possible variables, compositions of block copolymers were carefully controlled to ensure similar molecular weights. Table 1 summarizes the synthesized PDMS and block copolymers used in this study. Three different molecular weights of PDMS were prepared by controlling D_4/TMS ratios. We have shown earlier that block copolymers composed of PDMS and PMPC can be synthesized in a very well controlled manner by the ATRP method in protic media, even though both components display extremely disparate solubilities [26]. As shown in Table 1, three different compositions of block copolymers with similar molecular weights (determined by NMR) were successfully synthesized by the ATRP method. Unfortunately, not all polydispersity indices (PDI) measured achieved the appropriate low level (<1.3) because of the solubility problems. However,

because morphology of block copolymers is not that significantly affected by PDI, except in theoretical modeling [27], we considered compositions of block copolymers as variables only for the preparation of block copolymer templates.

3.2. Surface morphologies of block copolymer templates

The difference in solubility of each block plays a dominant role in the phase separation behavior of block copolymers. Because degree of immiscibility is determined by solubility parameters, block copolymers that contain two extremely different hydrophobic (PDMS) and hydrophilic (PMPC) parts are expected to form phase-separated structures easily.

Fig. 1 shows the bright-field TEM image of a block copolymer template stained with OsO_4. In PM1, no PDMS domains were
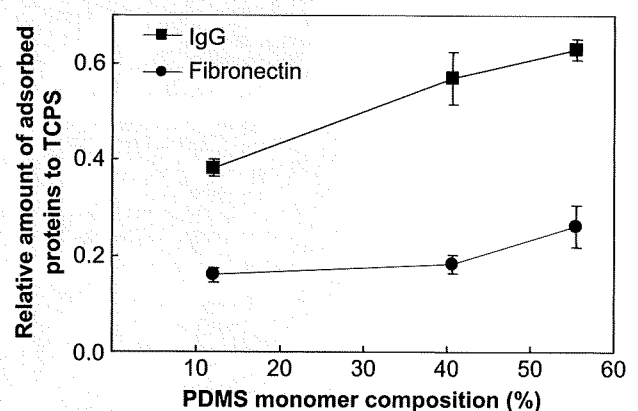

Fig. 7. Relative amount of adsorbed proteins on block copolymer surfaces as a function of PDMS compositions calculated by the micro-BCA™ experimental method. All values were normalized to the amount of adsorbed proteins on TCPS (=1).
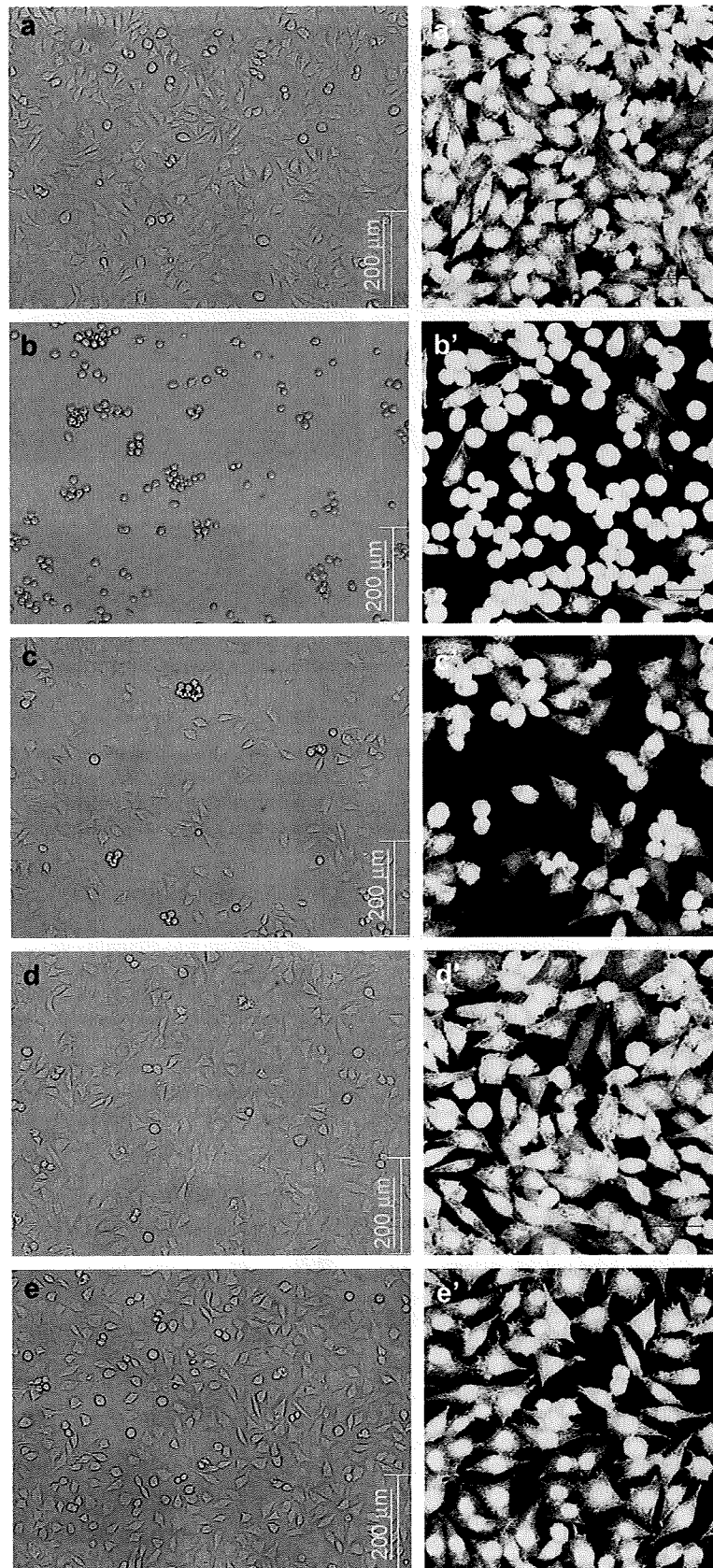
Fig. 8. Optical and confocal microscope images of L929 mouse fibroblasts after 2 days of cultivation on block copolymer surfaces in serum-containing medium. (a), (a') Noncoated TCPS; (b), (b') PM1; (c), (c') PM2; (d), (d') PM3; and (e), (e') PDMS (PDMS2-coated surface). Scale bar in optical image = 200 μm. Scan size of confocal images = 300 μm × 300 μm.

observed by TEM. This finding is probably because of the low level of the PDMS monomer composition, so that PDMS-core structure forms in a PMPC matrix, as illustrated. PM2 and PM3 exhibit cylindrical PDMS domain structures in a PMPC matrix with different domain sizes because of the high level of the PDMS monomer composition in PM3. Because cylindrical domain size can theoretically be controlled by PDMS monomer composition, this result agrees well with the molecular profile of the block copolymers.

Fig. 2A and B shows topological AFM images of block copolymers in a dry condition with different scan sizes. These AFM images agree well with the TEM images of Fig. 1 over a broad region, except for the individual domain sizes. Because measurement conditions for TEM and AFM are quite different, it is expected that these dimensions would not match exactly. However, the tendency shown in the AFM images that PDMS domain size increases, thereby allowing PDMS monomer compositions, agrees well with that of the TEM images. A similar tendency was also apparent in PBS.

Fig. 2C shows the AFM images taken in PBS. It is apparent that hydrophobic PDMS domain size increases as PDMS monomer composition increases. Morphological changes under wet conditions are possibly attributable to the swelled hydrophilic PMPC domain, which induces a significant increase in surface roughness (Fig. 3), which is an important variable for the determination of cellular responses. Difference in surface roughness between dry and wet conditions increases as PDMS monomer composition increased. This result indicates that the effect of a swelled hydrophilic PMPC domain on surface roughness increases when it coexists in nearly the same proportion as a non-swelled hydrophobic PDMS domain. This result is thought as schematically reasonable because the density of swelled/non-swelled domain is maximized when two domains coexist in nearly same proportion.

3.3. Surface characterization of block copolymer templates

Fig. 4 shows the quantitative influence of surface elements measured by XPS. In each block copolymer template, a strong phosphorus (P_{2p}) peak was detected at 134.0 eV and a strong silicone (Si_{2p}) peak was detected at 103.0 eV in different ratios. This P/Si ratio, calculated by peak integrals, continuously decreases as PDMS monomer composition increases. This finding indicates that the surface ratio of the PDMS domain increases as the PDMS monomer composition increases. This result corresponds well with the results from the earlier TEM and AFM observations. In contrast, the P/C ratios on the block copolymer surfaces have almost same value. This result is possibly due to the large amount of C_{1s} which detected in both PMPC and PDMS domains.

Fig. 5 shows results of static water contact angle measurement. It is apparent that hydrophobicity of block copolymer templates increases continuously as PDMS domain ratio increases. Nevertheless, it is also clear that all block copolymer surfaces showed a significantly low value of contact angle with regard to the PDMS surface (100% PDMS monomer composition), which had an approximately 95-degree static water contact angle. That is, even though the block copolymer template prepared by PM3 exhibits the maximum hydrophobic tendency among all the samples examined, the static contact angle of PM3 is only around 20°, so that there are enough hydrophilic surfaces such that homogeneously prepared MPC polymer surfaces are nonbiofouling in nature [28].

3.4. Biological responses on the block copolymer surfaces

3.4.1. Protein adsorption behavior

We investigated the effect of heterogeneous block copolymer surfaces on protein adsorption by TEM, using the micro-BCA™ experimental method with IgG and fibronectin as model proteins.

We used the IgG molecules labeled with 10-nm diameters of gold colloid so that their adsorption behavior could be observed easily by TEM. Fig. 6 exhibits the resulting TEM images of each block copolymer template after contact with IgG solution. In all the block copolymer templates, IgG molecules were selectively adsorbed only onto the hydrophobic PDMS domains. This result indicates that with phase separation, each block copolymer domain could retain its own biofouling and antibiofouling properties.

Similar phenomena for other block copolymer templates have been reported previously. For example, in an early study, Okano et al. proposed an interesting effect of block copolymer surfaces on protein adsorption behavior. They reported that a heterogeneously prepared block copolymer surface composed of hydrophilic poly-(hydroxyethyl methacrylate) (PHEMA) and hydrophobic PS induced preferential protein adsorption on each domain, thereby suppressing activation of adhered platelets [29]. Kumar et al. demonstrated selective protein adsorption on phase-separated block copolymer templates composed of PS and poly(methyl methacrylate) [30], and they also reported that such selective protein adsorption could also occur on more hydrophobic domains, even though the materials that comprise each block copolymer domain are all hydrophobic components [31]. However, all previously reported experiments were performed on surfaces that exhibit relatively high water contact angles (to the best of our knowledge, 50° as a minimum).

In our current study, we can confirm that heterogeneous MPC polymer surfaces derive selective protein adsorption even though these surfaces may have a very hydrophilic nature, i.e., a water contact angle of less than 20°. Because IgG is not a cell adhesive protein, we carried out a protein adsorption test by using fibronectin, another plasma protein that is involved in cellular adhesion.

Fig. 7 shows the amount of adsorbed proteins determined by the micro-BCA™ method. It is apparent that the adsorption tendency of fibronectin is similar to that of IgG; that is, the amount of adsorbed protein depends on the hydrophobicity of the surfaces. Unfortunately, because of technical problems, direct observation of fibronectin adsorption was not possible. However, we expect that adsorption behavior of fibronectin would resemble that of IgG, because selective fibronectin adsorption occurred only onto the PDMS domains.

3.4.2. Cell adhesion behavior

We studied cell adhesion behavior on block copolymer templates by using L929 mouse fibroblast cells. Fig. 8 depicts
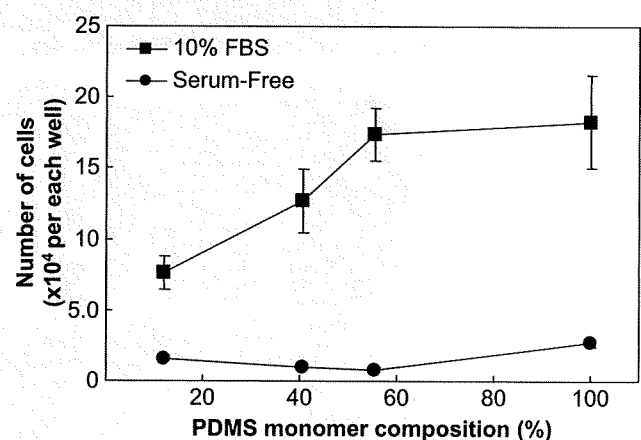

Fig. 9. Number of cells on block copolymer surfaces after 4 days of cultivation as a function of PDMS composition. One hundred percent indicates the PDMS2-coated surface as a negative control.